Laser-hybrid Accelerator for Radiobiological Applications (LhARA)

John Adams Institute Accelerator Design Project 2024

M. Pereira, G. Passarelli
Royal Holloway, University of London

C. Jolly, S. Leadley, C. Lehmann, S. Preston
University of Oxford

G. Christian, L. Bradley, J. Hills, L. Kennedy
Imperial College London

This Project

- Part of the annual project for 1st year PhD / DPhil students within the John Adams Institute for Accelerator Science, concluding our accelerator physics coursework.
- Collaboration between 10 students across 3 universities, over the course of the first 3 months of 2024.
- Had weekly meetings with Will Shields and Ken Long (and many others!) to discuss progress and allocate tasks.
- The overall aim is to investigate some finer details on LhARA Stage 1, specifically around:
  - Lattice Optimisation
  - RF Cavity Design
  - Magnet Design

John Adams Institute for Accelerator Science

ROYAL HOLLOWAY UNIVERSITY OF LONDON

Imperial College London

UNIVERSITY OF OXFORD

Motivation

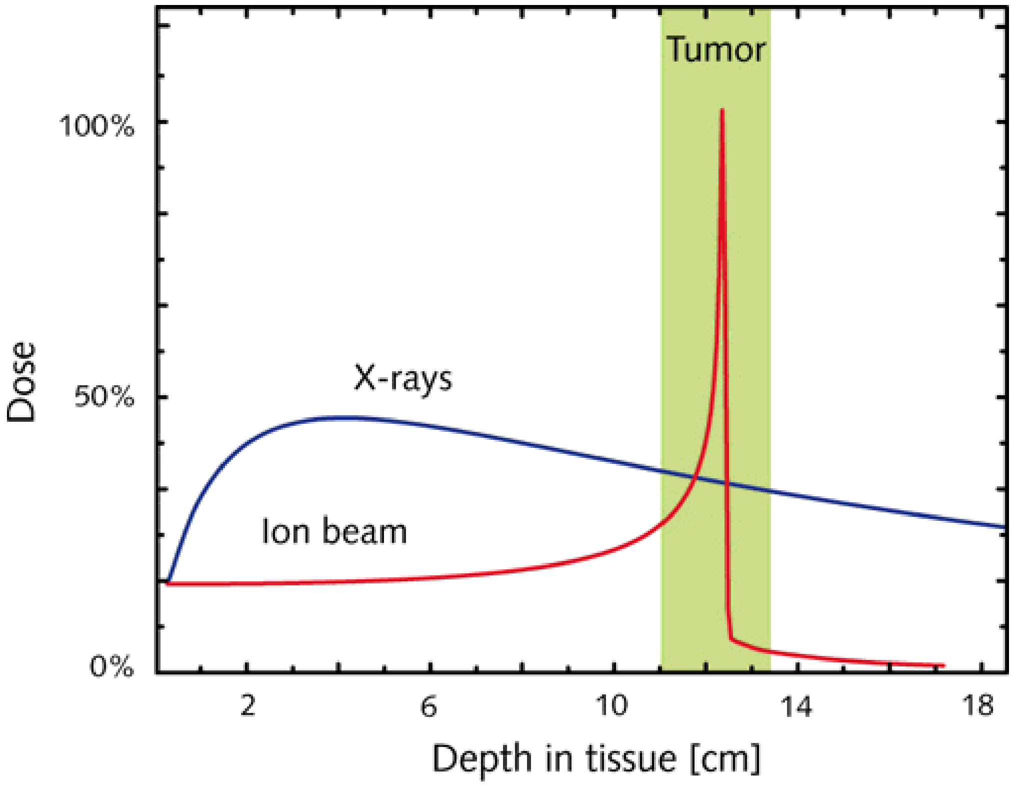

[1] Comparison of radiation dose as a function of depth.

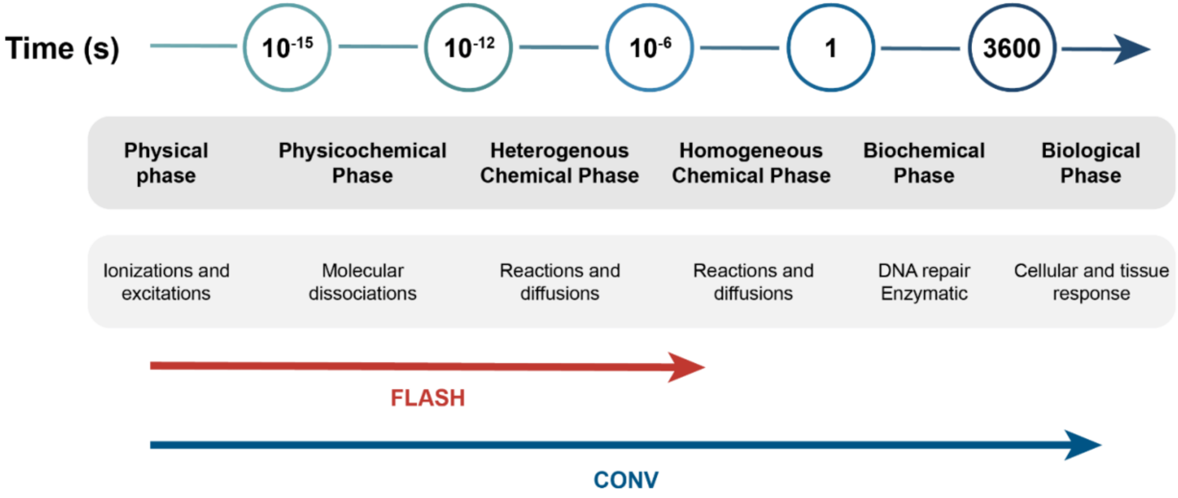

[2] Flash timescales compared to conventional RT

- Development of more accessible, cheaper alternatives for RT (radiation therapy)
- Study of ion beam radiobiology
- Exploration of novel treatment modalities

Introduction

LhARA (Laser-hybrid accelerator for radiobiological applications)

Beam Parameters

- Energy
- Ion species
- Dose, dose spatial distribution, dose rate
- Biological end point

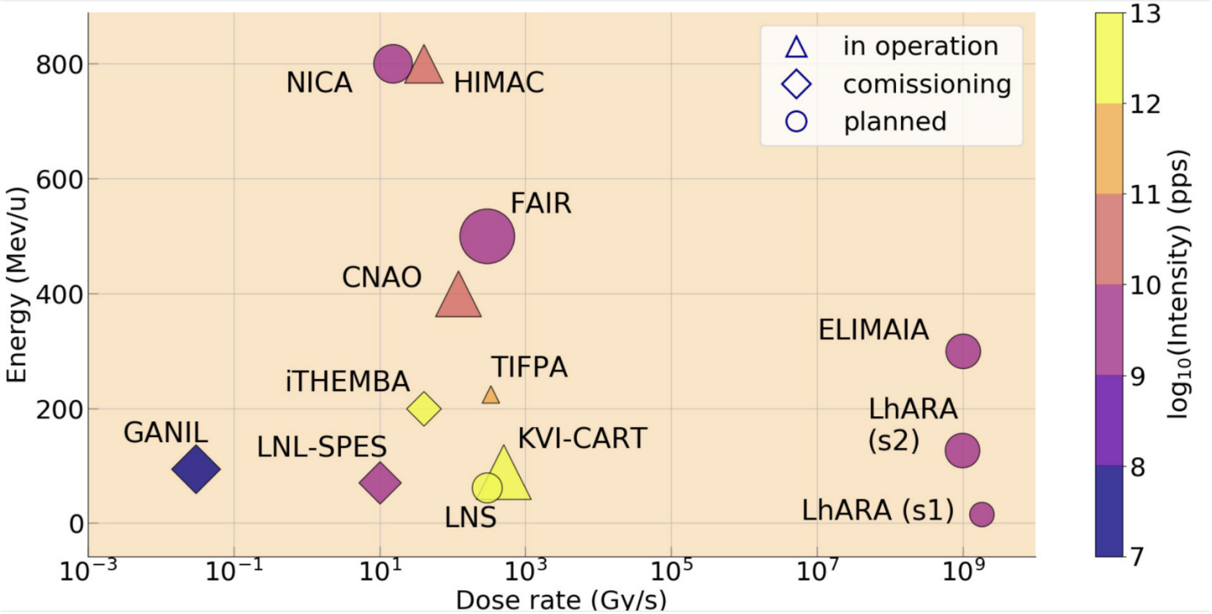

[3] Facility comparison showing where the planned LhARA S1 & S2 are in energy & dose rate.

Target Normal Sheath Acceleration (TNSA): Exploration of Hybrid Acceleration

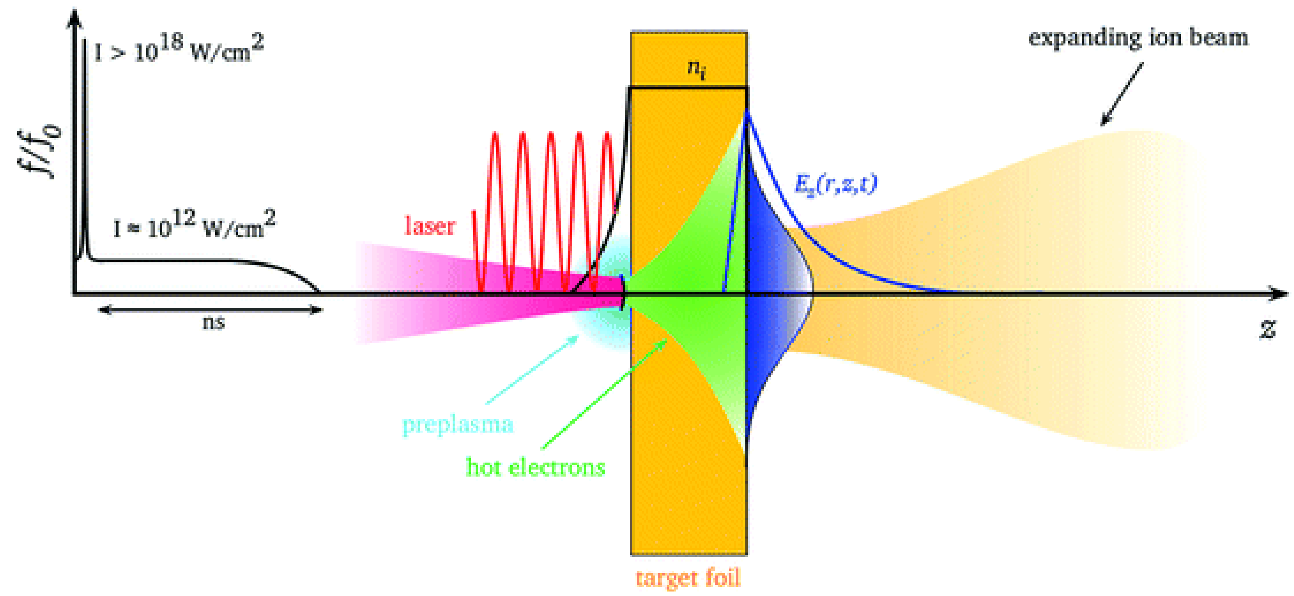

[4] Solid target interaction using TNSA to produce proton beams

Parameter	Value or range	Unit
Laser power	100	TW
Laser energy	2.5	J
Laser pulse length	25	fs
Laser rep. rate	10	Hz
Proton energy	15	MeV

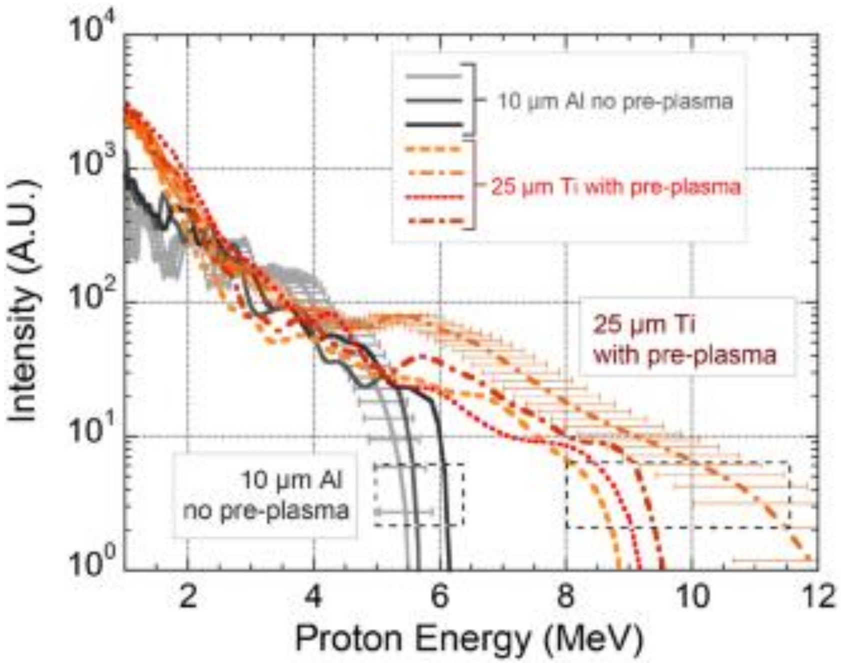

[5] Ion beam spectra characteristics

Introduction

Gabor Lenses

Advantages

- More efficient focusing compared to high-field solenoid
- Reduces costs
- Focus in both planes simultaneously
- Variable focusing strength proportional to plasma density

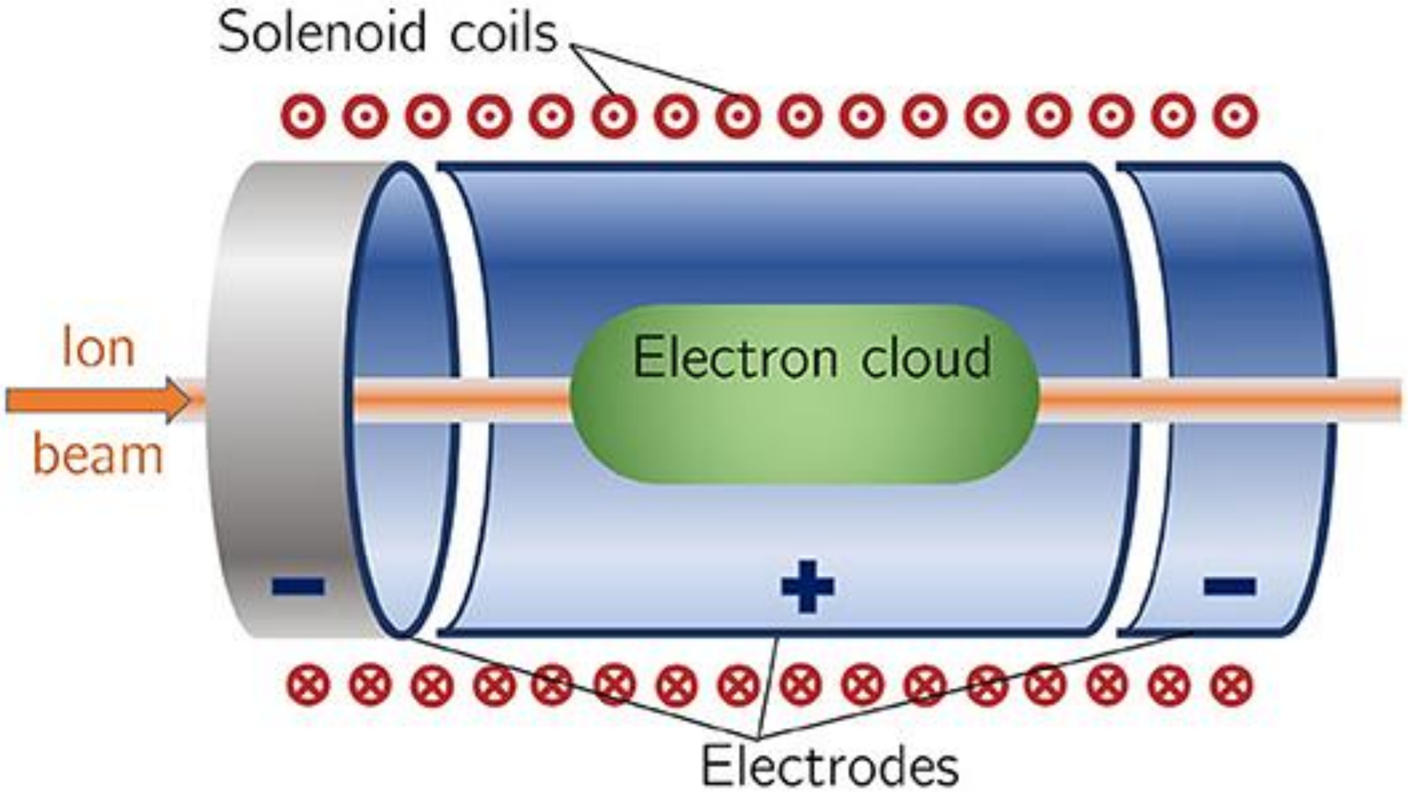

[6] Schematic of Gabor Lens to be used in LhARA

LhARA Design Overview

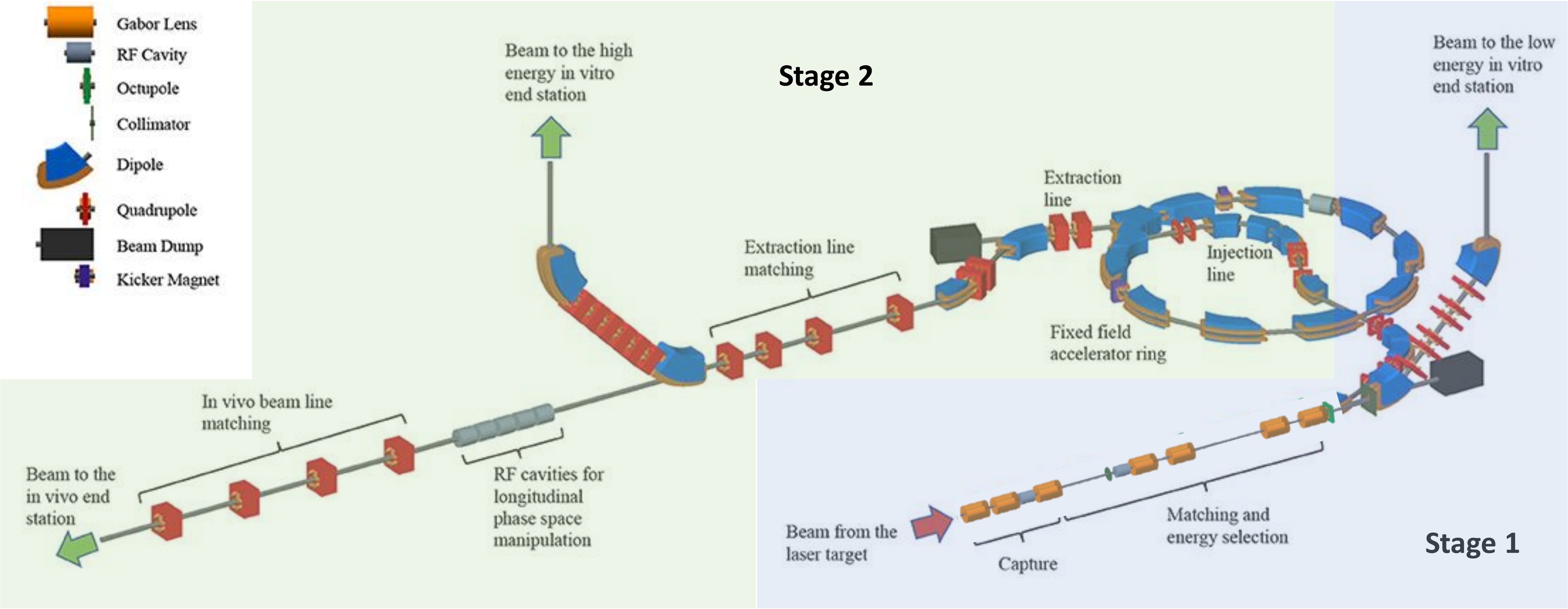

[7] Proposed LhARA facility.

Introduction

End Station Specifications

Low energy (in vitro)

1. Low uniform dose distribution (<5%)
2. Minimal beam losses
3. Maximized dose delivery
4. Maximum diameter 1-3cm or focused down to 1mm
5. 12-15 MeV

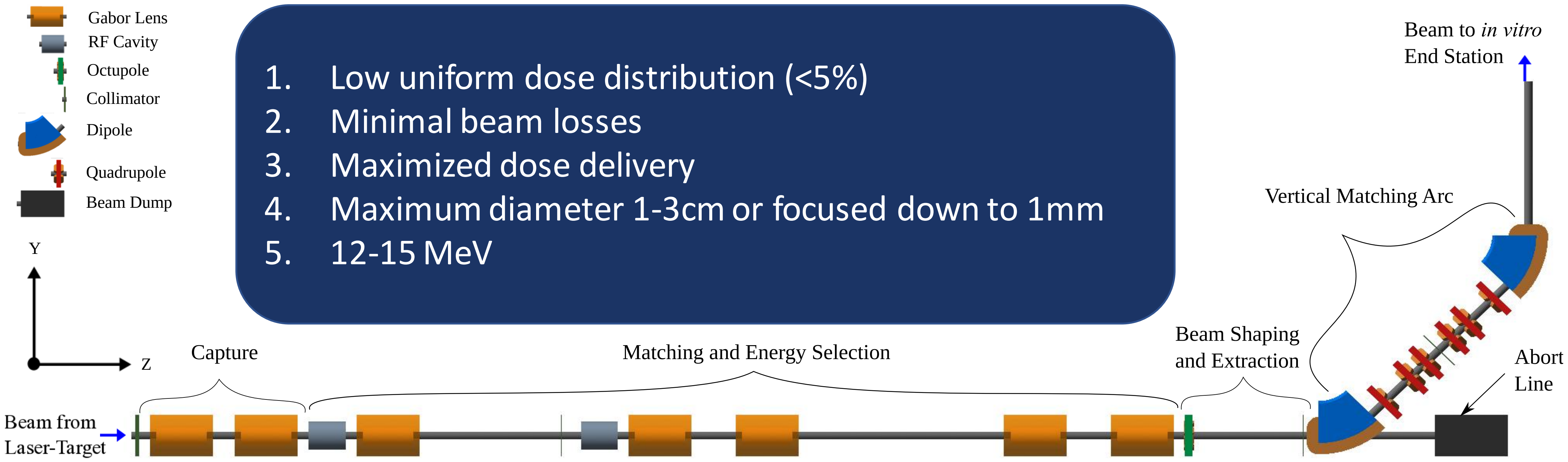

High energy (in vivo and in vitro)

1. Variable Injection energy using stage 1 beam line focusing strengths allows variable proton energies
2. 15 MeV -127 MeV

Lattice Design

Gregory Christian (gregory.christian.22@imperial.ac.uk)
Imperial College London
Jasmin Hills (jasmin.hills19@imperial.ac.uk)
Imperial College London
Lewis Kennedy (l.kennedy23@imperial.ac.uk)
Imperial College London
Matt Pereira (matthew.pereira.2023@live.rhul.ac.uk)
Royal Holloway, University of London
Shaun Preston (shaun.preston@physics.ox.ac.uk)
University of Oxford

Lattice Constraints

1. Beam focus after Lens 3 (S = 5.5m)
2. Twiss alpha -> 0 between Gabor lenses 2-3
3. High dispersion and low Twiss beta in the arc
4. Twiss alpha and dispersion -> 0 at end station
5. Low twiss beta (spot size)

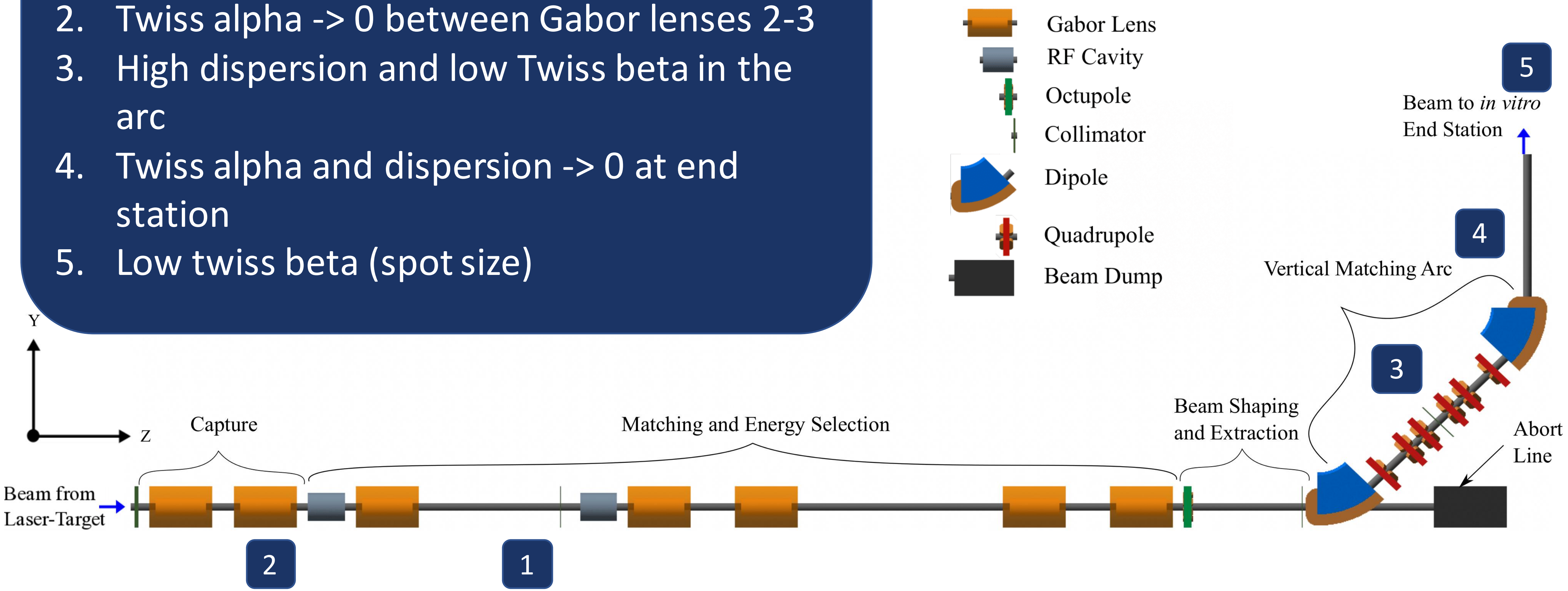

Lattice

Beam Size Optimisation – 3.0cm Configuration

Methodical Accelerator Design (MAD-X)

- General purpose accelerator design tool with a focus on beam dynamics and optics optimisation

1. Beam focus after Lens 3 (S = 5.5m)
2. Twiss alpha -> 0 between Gabor lenses 2-3
3. High dispersion and low Twiss beta in the arc
4. Twiss alpha and dispersion -> 0 at end station

To keep constraint 1 satisfied for all configurations, only lenses 4-7 were varied to achieve smaller spot sizes.

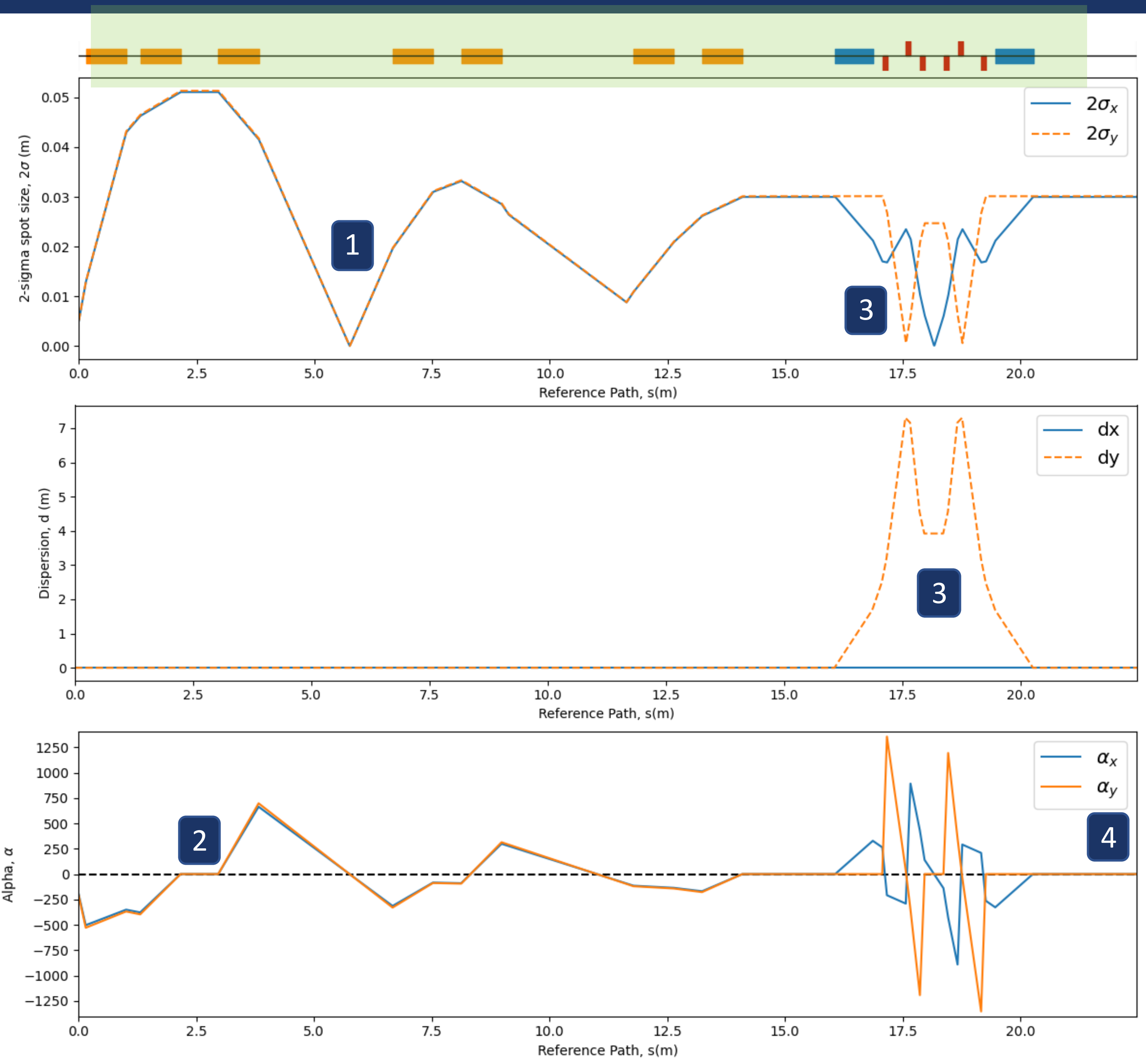

Lattice

Beam Size Optimisation – MAD-X Solenoid Matching

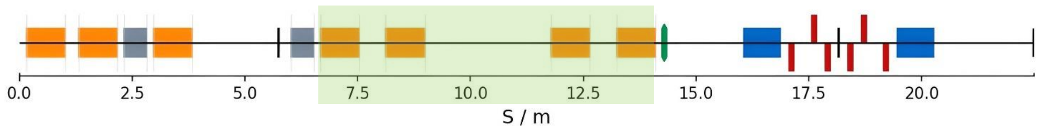

MATCH module used to vary solenoid strengths and apply lattice constraints to find lower spot size configurations

	Solenoid Strength, K_S			
2σ Spot Size (cm)	Lens 4	Lens 5	Lens 6	Lens 7
3.0	1.80	1.61	1.24	1.91
2.0	1.94	1.48	1.82	0.65
1.0	1.93	1.33	2.49	0.88

Beyond 1.0 cm, MAD-X is unable to accurately reach the intended beam size AND sufficiently satisfy lattice constraints in Dispersion and Twiss Alpha

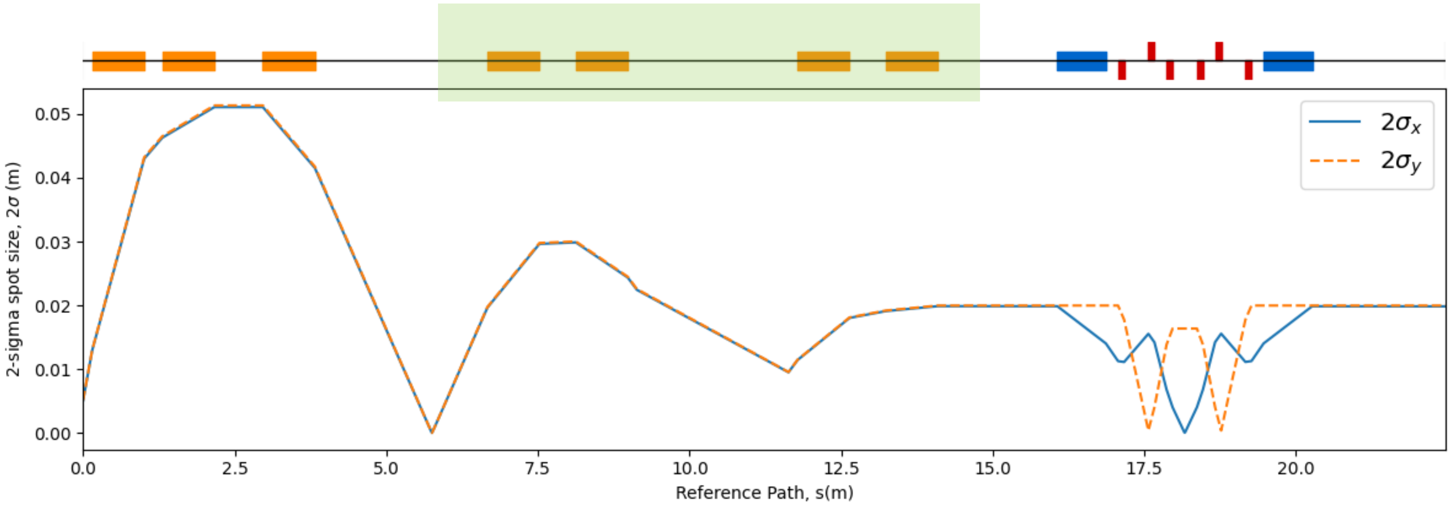

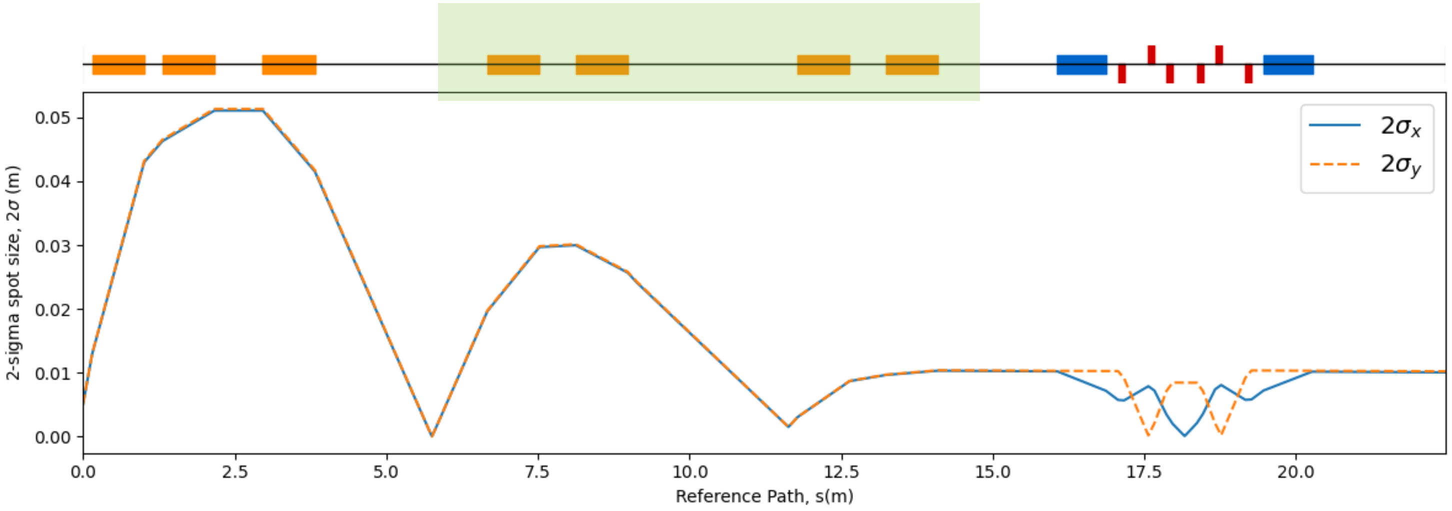

Lattice

Arc Optimisation - Quadrupole Strength

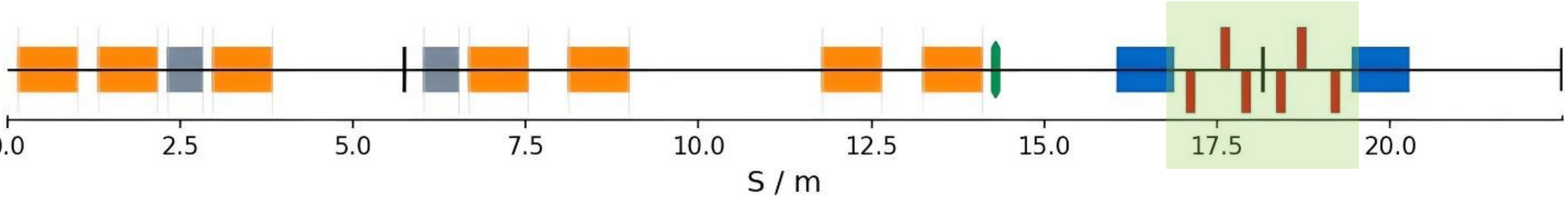

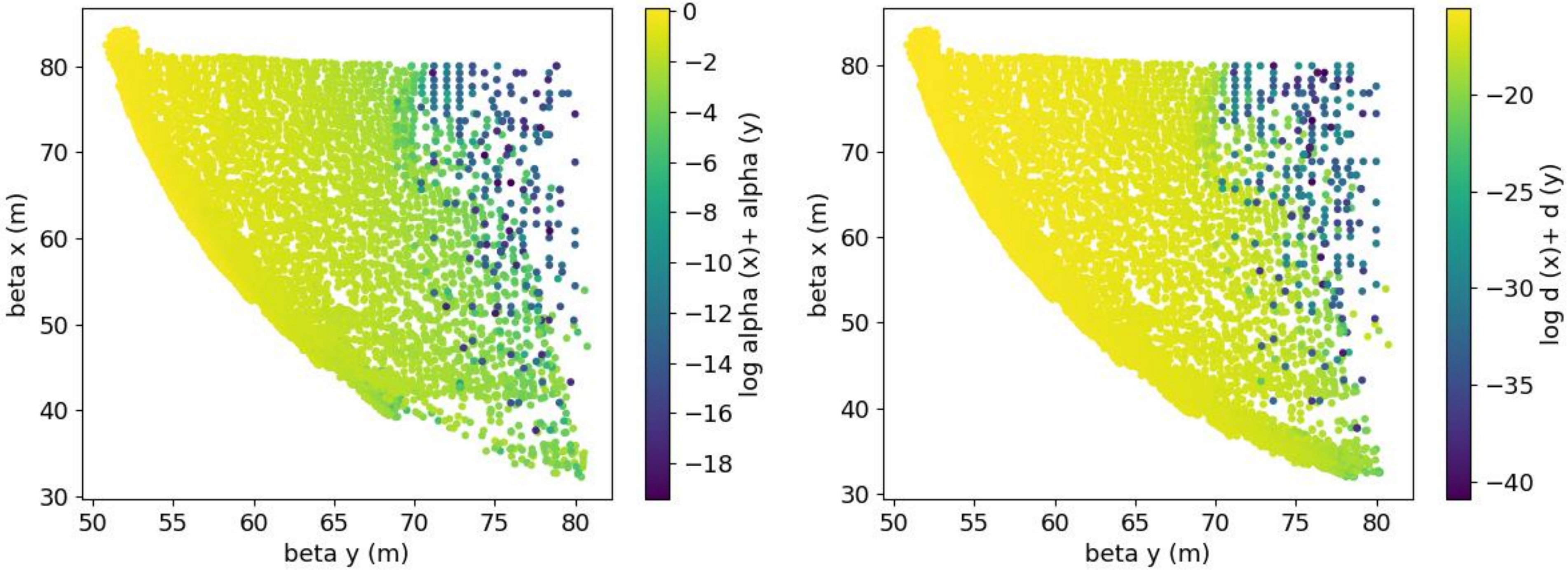

Alpha and dispersion for a variety of beta values

Required strengths: -21.9, 31.2, -32, -31.1,31.5, -23.3 [1/m]

BDSIM Lattice Model

Beam Delivery Simulation (BDSIM)

- Program utilising the Geant4 physics libraries to simulate the transport of a particle beam through a 3D model of the accelerator with realistic physics processes.

Studies on the BDSIM Lattice

- Energy loss and deposition along the beamline
- Dose rate calculations
- Beam uniformity through the octupole
- Gabor lens performance study (vs solenoids)
- Tracking through a 3D field map of the student designed RF cavity.

Studies on the BDSIM lattice use a 3.0 cm beam size to account for:

- BDSIM not including the effects of space charge
- The largest beam size being most effective for studying losses

[8]

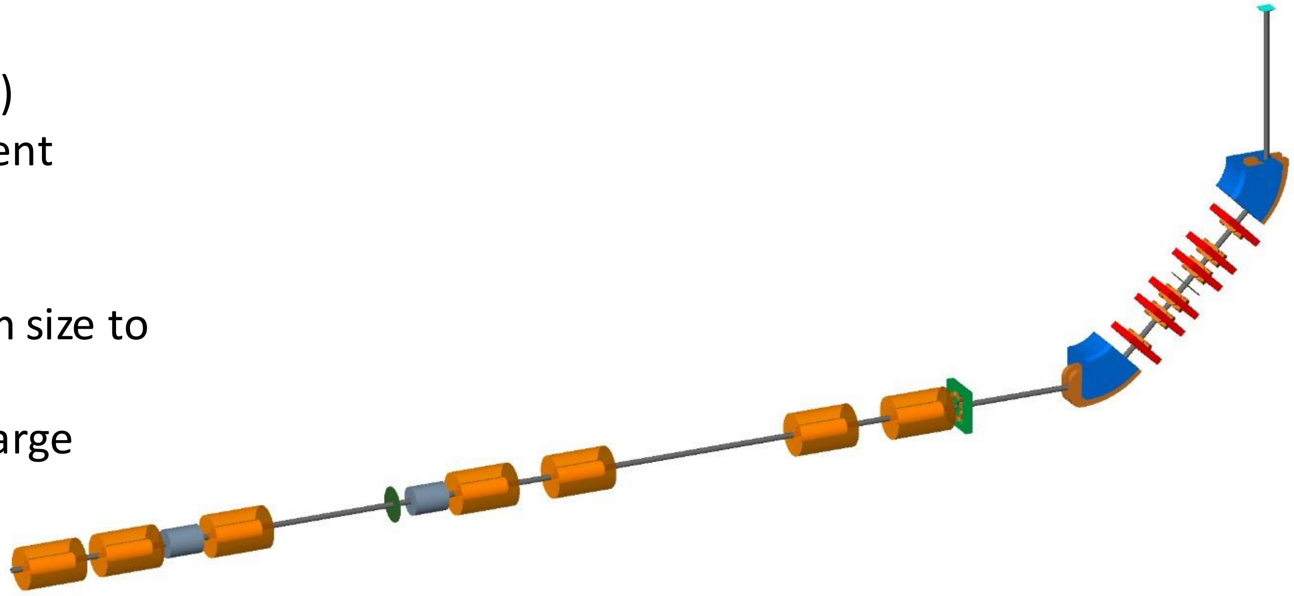

Beam and Energy Loss

Solenoid run with 10000 protons excluding collimators

A Global aperture radius of 3.65cm was found to minimize total beam loss across the lattice.

The "g4QGSP_BIC_EMZ" Geant4 physics list was used for simulation. Chosen as it is most common for handling physics for radiobiology/medical applications.

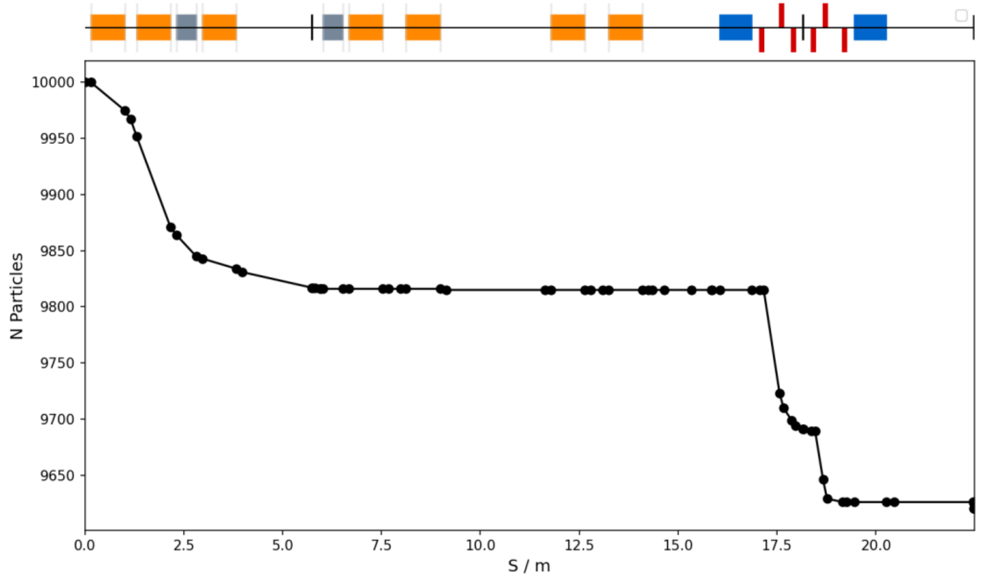

Energy and Deposition plot under the same conditions with 10 million protons.

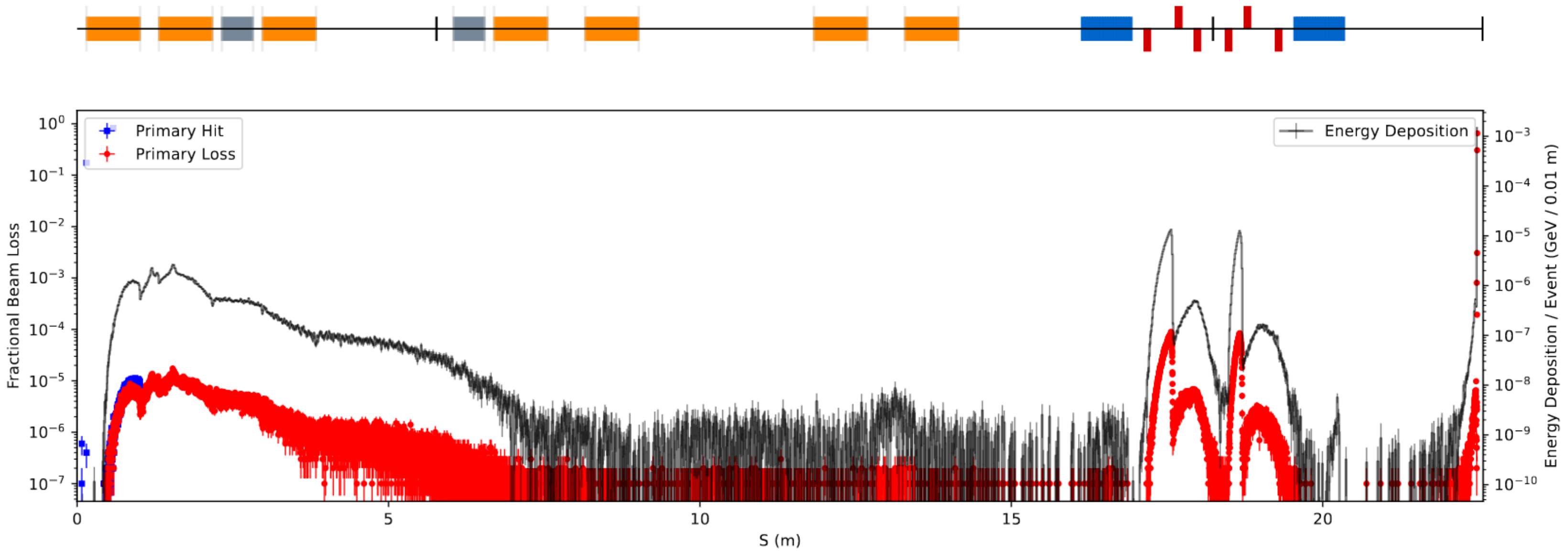

Lattice

Beam and Energy Loss

Collimator 1 – After GL3
- **Energy Cleaning**
- Positioned where the beam is at its smallest
- Circular aperture
  - Radius of 1.8mm (~2σ)

Collimator 2 – Middle of Vertical Arc
- **Momentum Cleaning**
- At the point of maximum Dispersion
- Elliptical aperture
  - Y-width of 1.2cm (~2σ)
  - X-width of 2.0cm
- Particles lost in dispersive y-axis, minimal losses in x.

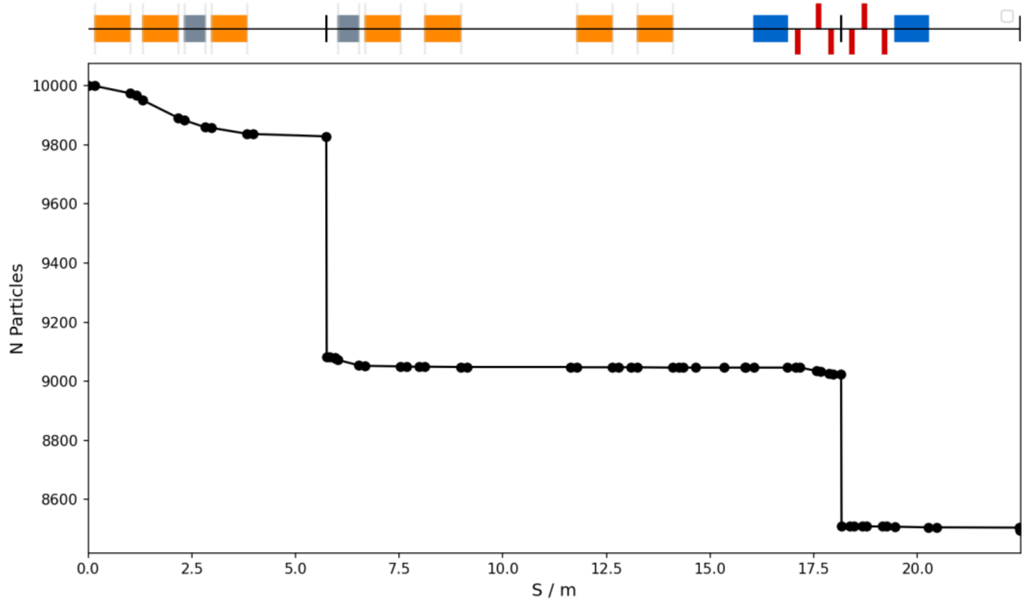

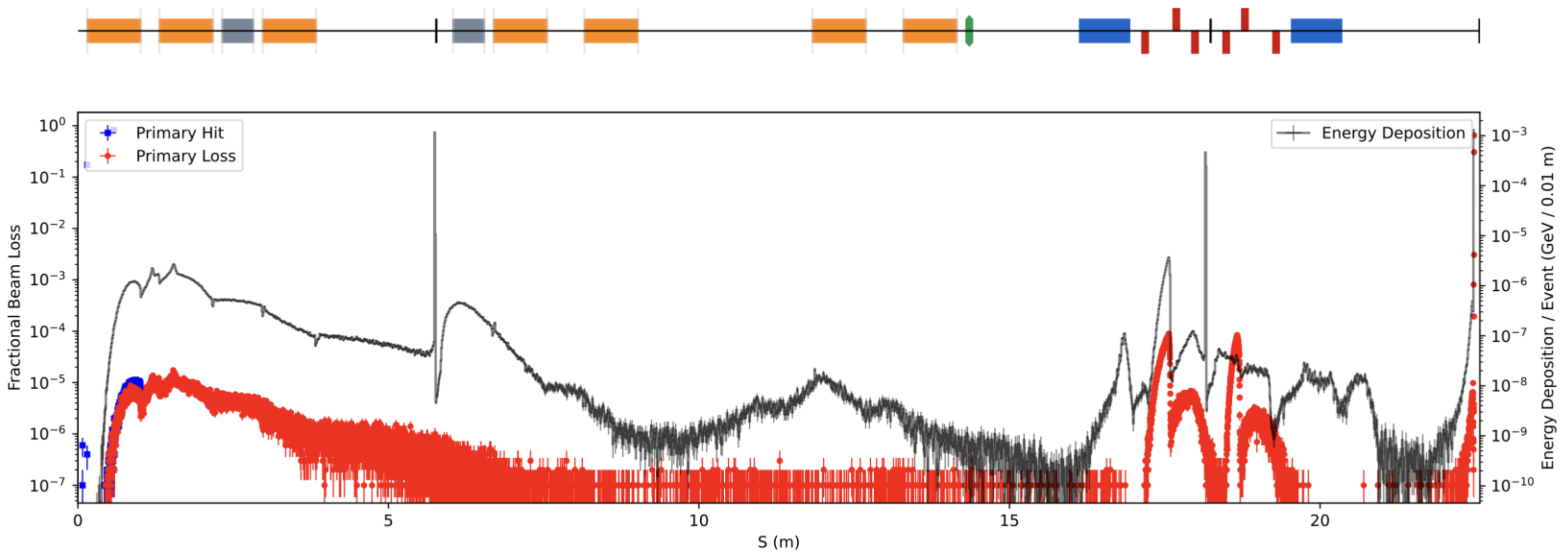

Stage 1 End Station in BDSIM

To enable **Dose Calculation**, a model end station target is placed at the end of the stage 1 lattice.

Dose is scored in a cylindrical volume within the water comparable to a Markus ion chamber
r = 2.65 mm

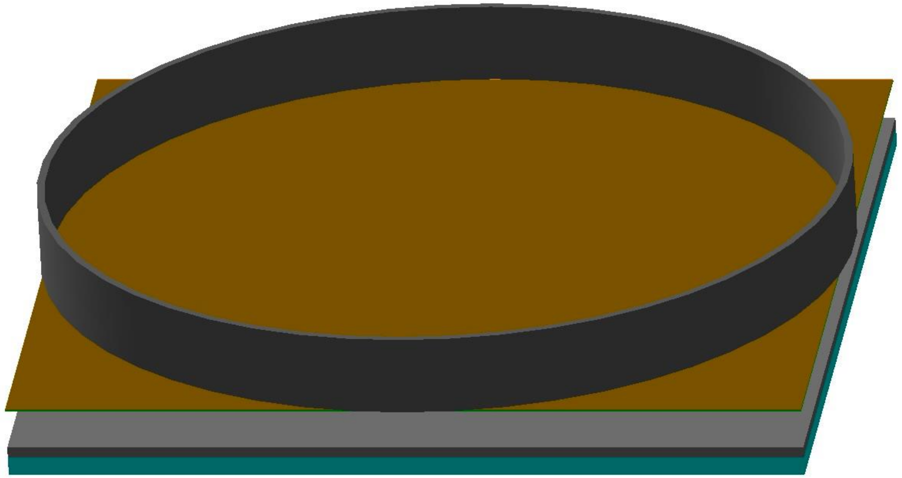

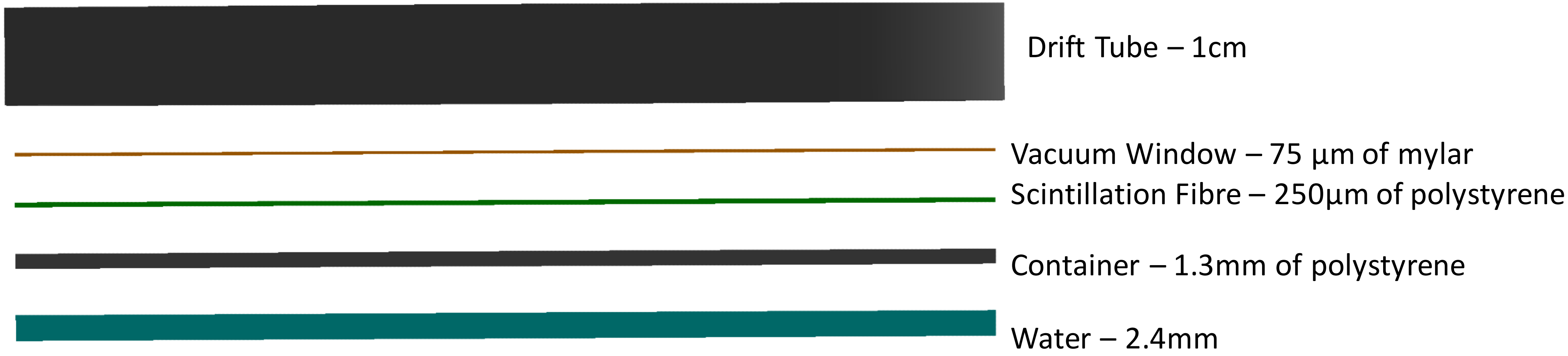

Lattice

Dose Rate for 1cm beam directly into end station (no losses) = 122.63 ± 1.41 Gy/s
Close to LhARA's theoretical maximum dose rate in literature (~120 Gy/s) [7]

Dose Rate Calculation

Dose Rate Calculation:

- Dose per proton extracted from the scorer and scaled by a factor of 10^{10} to represent the expected 10^9 particles per shot and the 10 Hz repetition rate of the laser

	Dose Rate (Gy/s)	Change w.r.t Reference (Gy/s)
Reference	17.42 ± 0.01	n/a
3.65cm Aperture	17.15 ± 0.02	-0.27
w/ Collimator 1	16.73 ± 0.03	-0.69
w/ Collimator 1+2	15.12 ± 0.01	-2.30

More significant impact of the second, **Momentum Cleaning**, collimator validates the design choices as this collimator is intended to do the "heavy lifting" when it comes to necessary losses to ensure a parallel beam at the end station.

Motivation for Smaller Beams
Smaller beams will experience less loss along the beamline and see more of the scoring region of the end station model, correlating to a higher calculated dose rate.

Octupole Tracking – Beam Transfer through Stage 1

10,000 particles through the beamline …

Octupole ***Selection Arc***

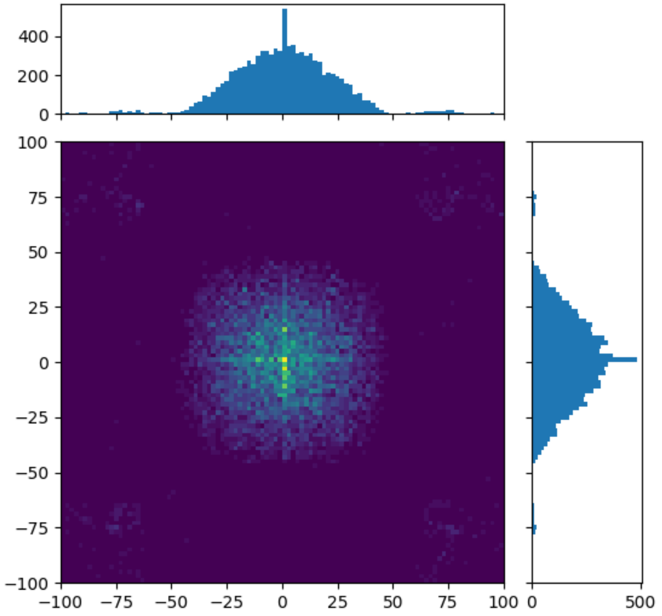

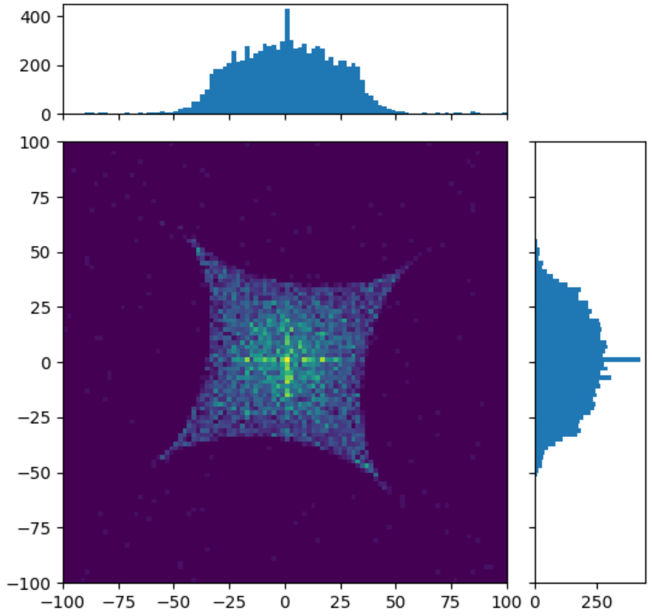

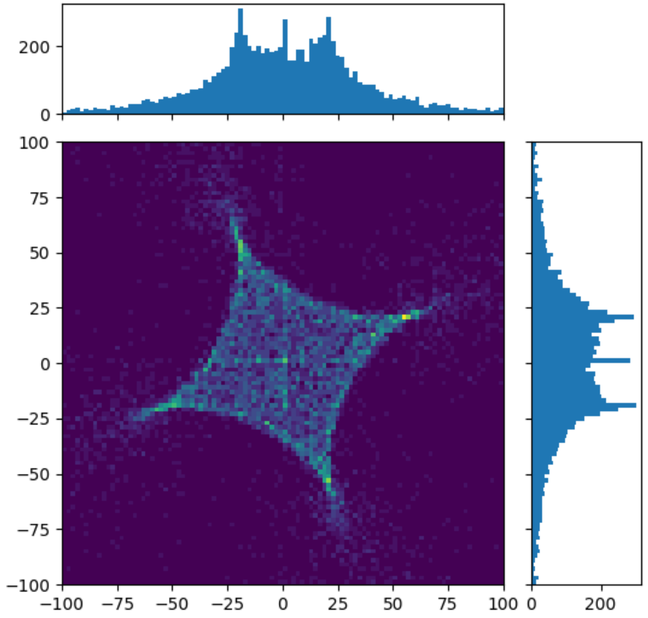

Lattice

Octupole: Capturing Missing Trends and Data

A quantile-quantile (QQ) plot directly compares the quantiles of two distributions to check for similarity. When one of those distributions is theoretical, we have what is known as a probability plot.

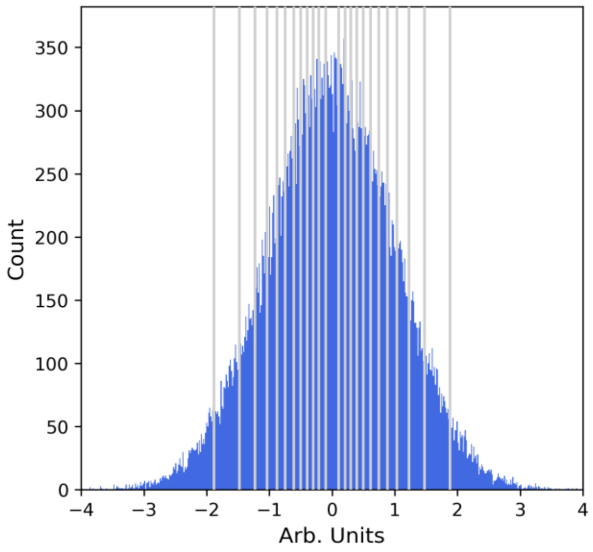

generates

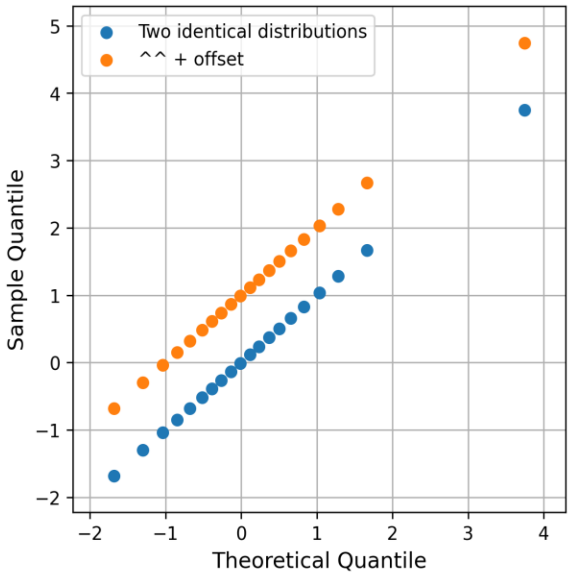

Lattice

Octupole: Capturing Missing Trends and Data

Applying this to the octupole data …

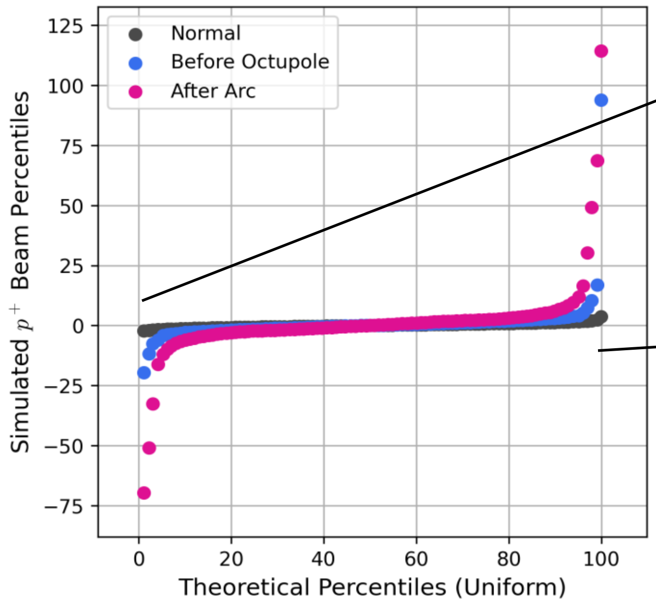

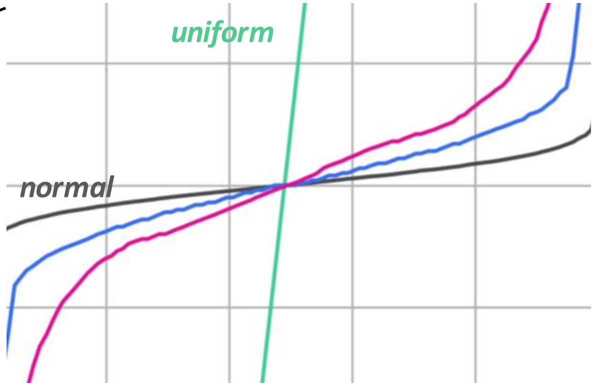

R1 = 0.60

R2 = 0.45

Outcome:

- Larger coefficient = better uniformity.
- Full distribution captured.
- Beam-beam comparisons possible.

Lattice

Gabor Lens Comparison

Performance study between solenoid and Gabor lens models in BDSIM

Confinement field neglected (~0.03T solenoid)

Plasma magnetic field negligible at proposed densities (~5e15 m^{-3})

Modelled as drift elements with field maps and scaling applied

Requires sufficient plasma density/uniformity to neutralise beam space charge and avoid instabilities

$$E_r = -\frac{e n_e r}{2\epsilon_0}$$

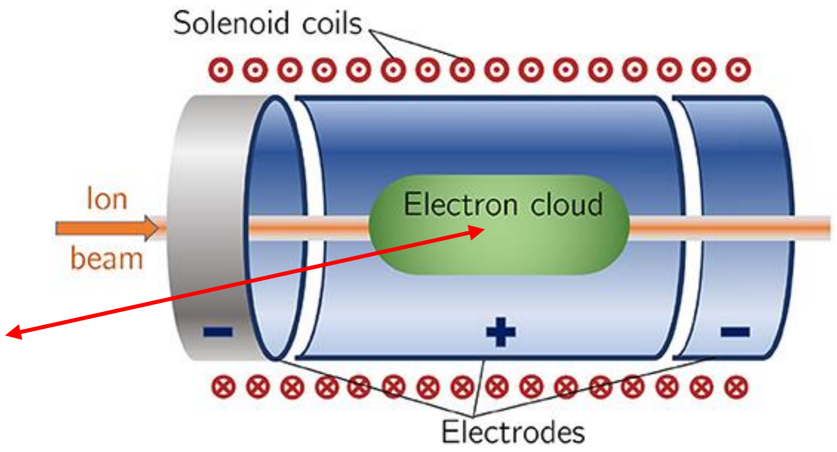

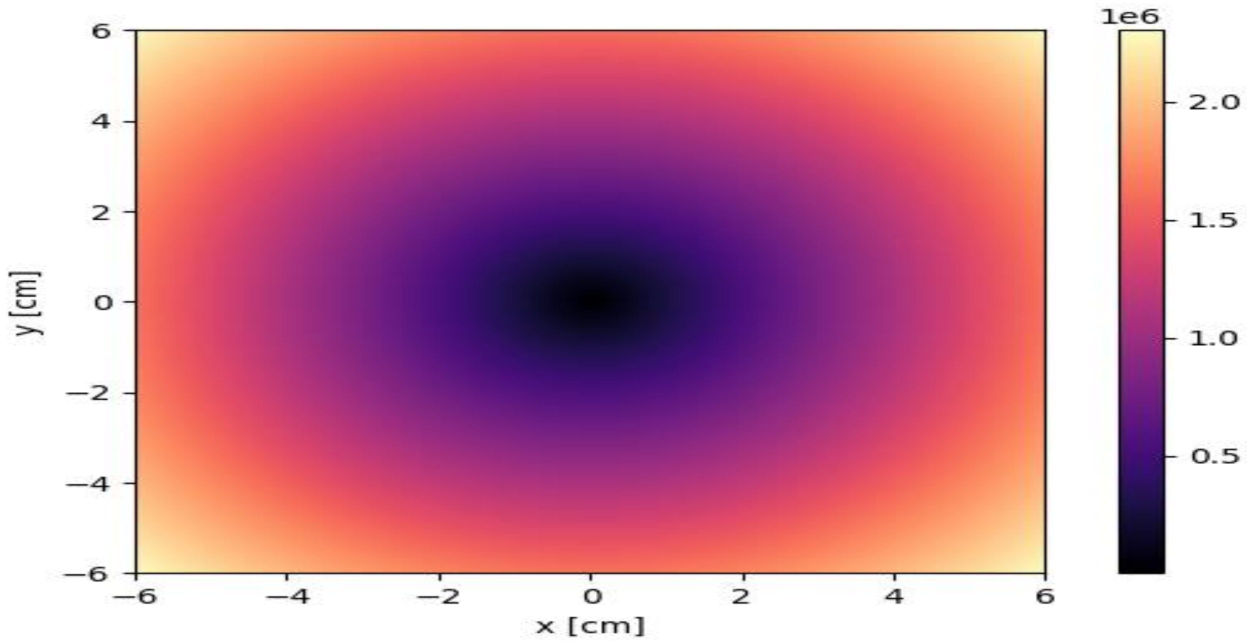

Field map equivalent to 1T

Lattice

Gabor Lens Comparison

COBYLA optimisation for fine tuning optics [9]

Constraints remain satisfied

Solenoid strengths: 1.40, 0.57, 0.80, 1.04, 0.80, 1.40, 0.28

Gabor lens strengths: 1.38, 0.56, 0.81, 1.04, 0.80, 1.38, 0.32

Comparable strengths, same optics but much less power required

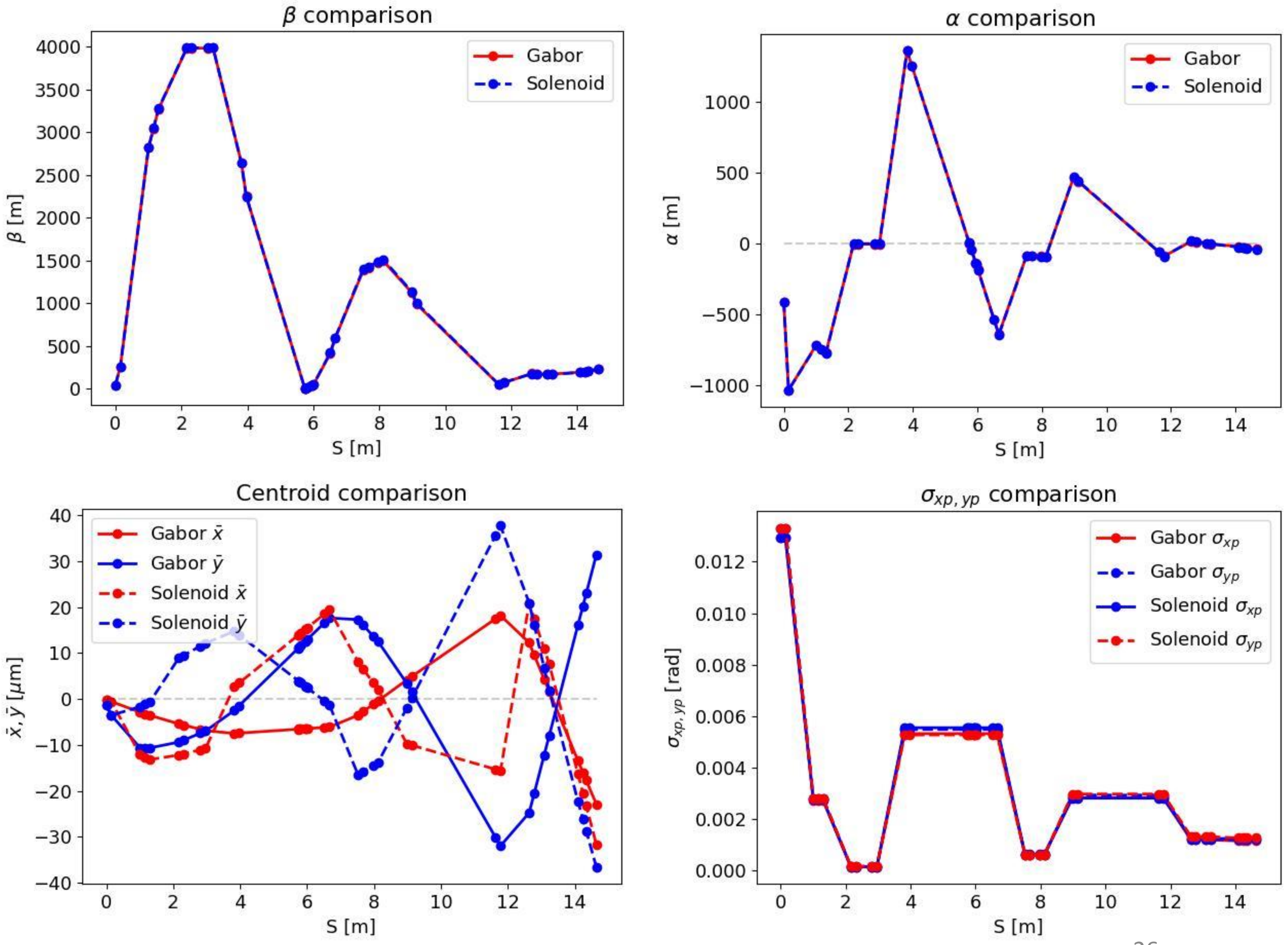

RF Cavity Design

Giusy Passarelli (giusy.passarelli.2024@live.rhul.ac.uk)
Royal Holloway, University of London
Corey Lehmann (corey.lehmann@physics.ox.ac.uk)
University of Oxford
Carl Jolly (carl.jolly@physics.ox.ac.uk)
University of Oxford

RF Introduction and Requirements

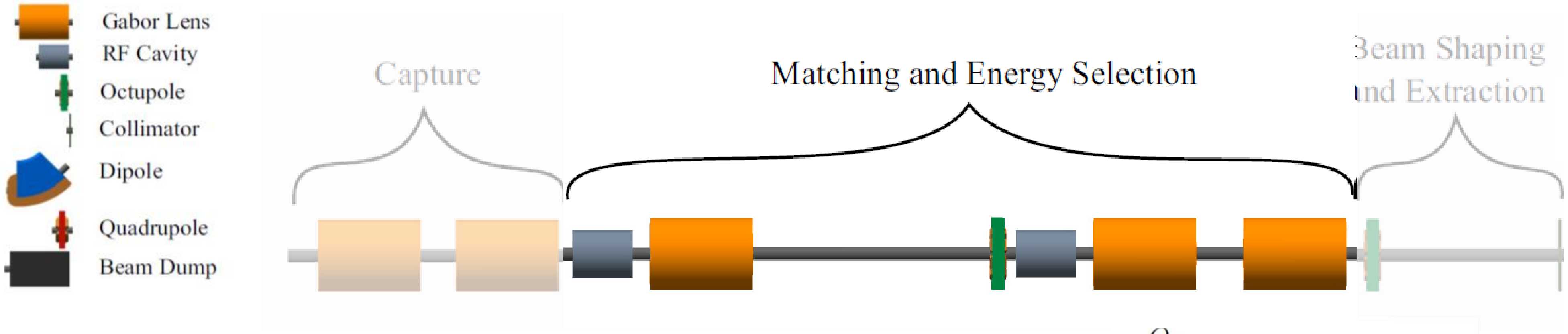

RF Cavity permits:

- Control of **bunch length;**
- Manipulation of the **longitudinal phase-space.**

$$V_{RF} = \frac{\Delta E^2 \pi h |\eta|}{2 q \beta^2 E_s}$$

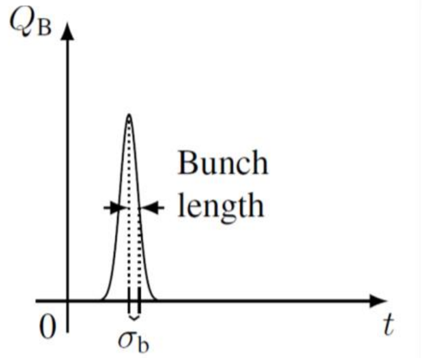

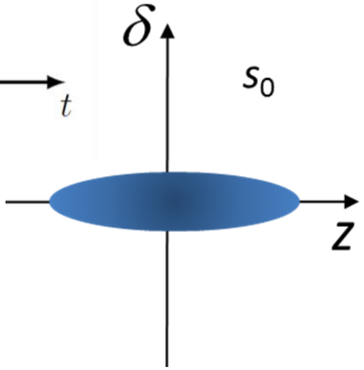

RF Cavity Requirements:

- Beam Energy = 15MeV
- Total relative energy spread = ± 2%
- Initial bunch length ~ 10 fs
- Distance between the beam source and the first RF Cavity ≅ 3m

Frequency Choice

- RF frequency tuned for bunch length alignment on rising RF wave edge.
- Late particles (closer to the bunch end) gain energy, while early ones (closer to the beginning) lose it, ensuring **phase stability**.
- All particles receive a positive acceleration at the same time, and the beam remains grouped throughout its trajectory.

Frequency	Bunch Length "Stability"
201 MHz	2.5 ns
352 MHz	1.4 ns

- Energy spread > 2% ⇒ Frequency < 201MHz

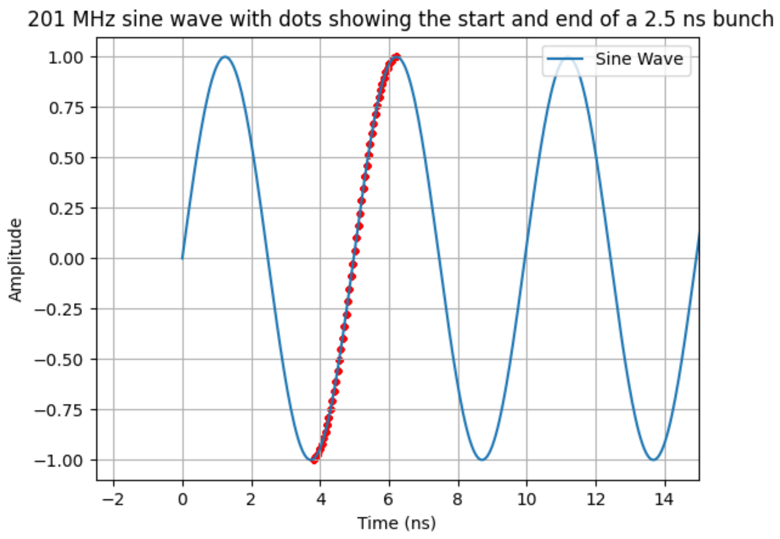

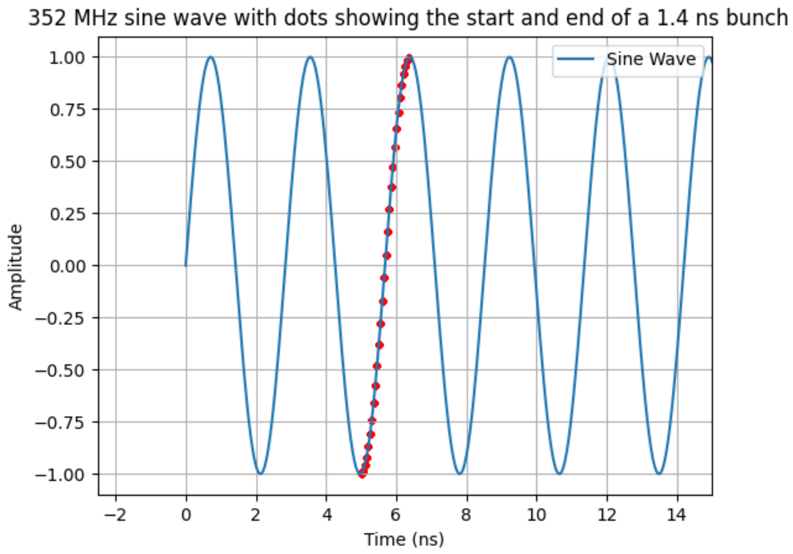

Important Definitions

Kilpatrick Factor

- Used to indicate how close a cavity is to electric breakdown for a given field and frequency.
  - Originally breakdowns occur at Kilpatrick factor of 1. Now we commonly design for 1.5

Shunt Impedance

- Indicates how efficiently RF power is converted into an accelerating voltage
  - Higher is better

Transit Time Factor

- Indicates how much of a uniform field the particle sees as it transits the cavity. 1 is uniform acceleration, 0 is no acceleration.
  - High Transit time factors are typically better

SuperFish CCL Geometry

8 Free Parameters:

- **Length**
- **Gap Length**
- Outer Corner Radius
- Inner Corner Radius
- Outer Nose Radius
- Inner Nose Radius
- Flat Length
- Cone Angle

Automatically adjusts diameter to fit frequency

Automatically adjusts E field to reach Kilpatrick factor of 1.5

Optimising for:

- Shunt Impedance
- Transit Time
- **Bunching Capability**

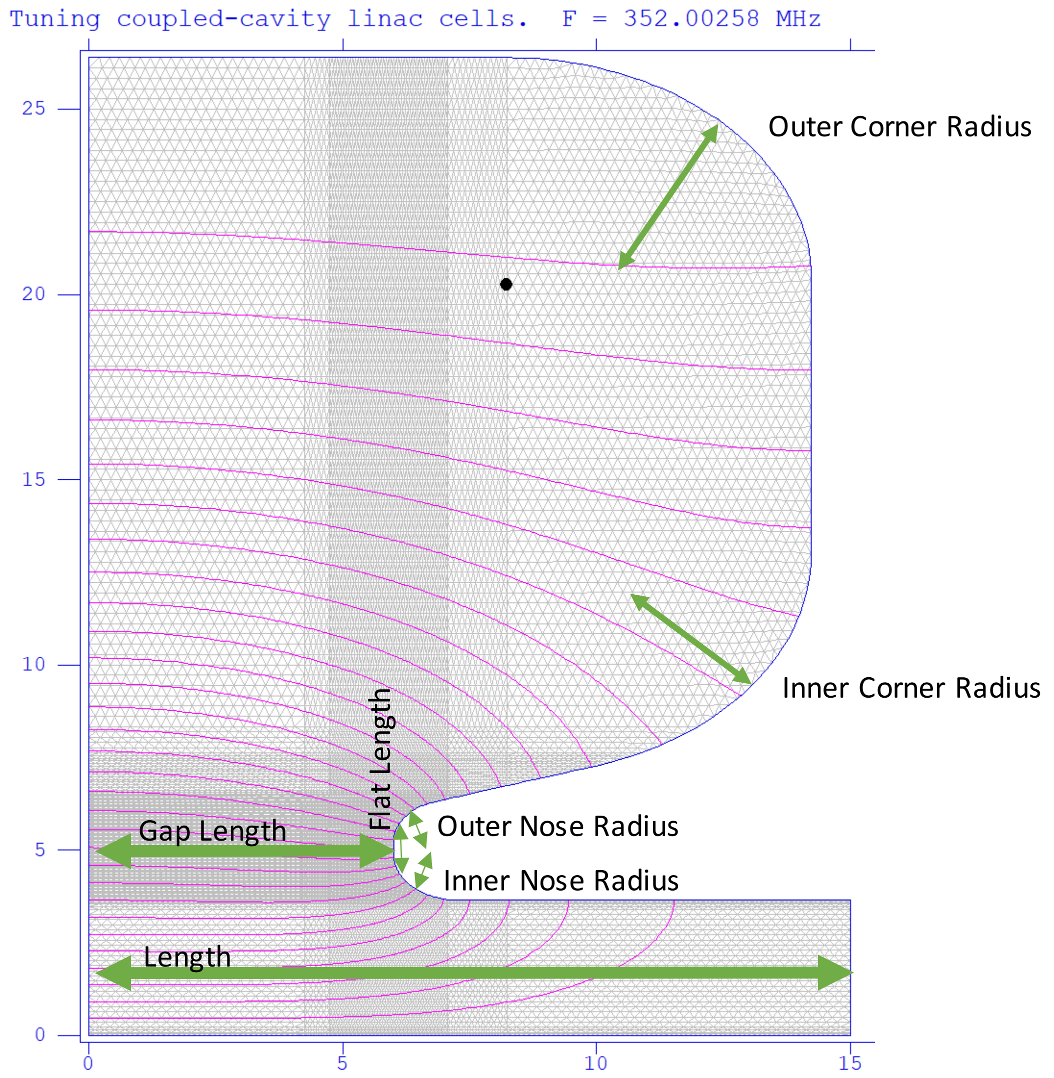

Cavity Optimisation

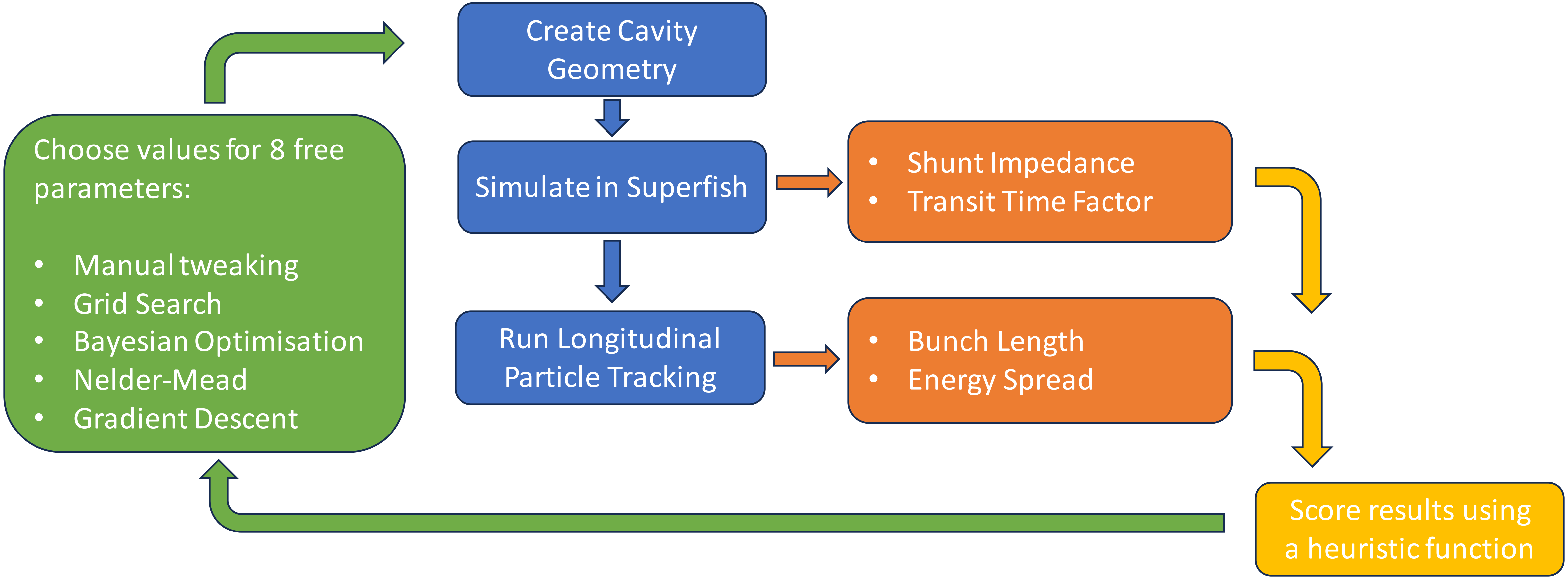

Longitudinal Particle Tracking

Need a way to measure bunching ability for each cavity design.

- Write a simple particle-tracking simulation code
- Generate N particles representing bunch distribution
- Treat most of accelerator as drift
- On passing through the RF cavity, change the energy of the particle based on the field profile calculated in SuperFish
- Record the bunch length and energy spread at exit

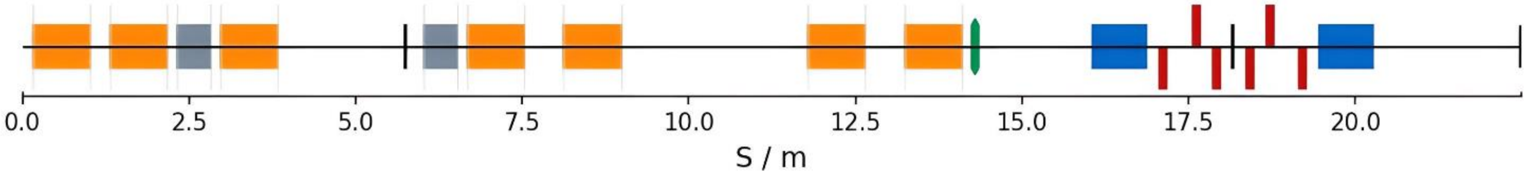

Longitudinal Phase Space Simulation – Cavities OFF

Energy: 15 ± 0.29 MeV (1.92%)
Bunch Length: 0.82 ns

15 MeV Protons

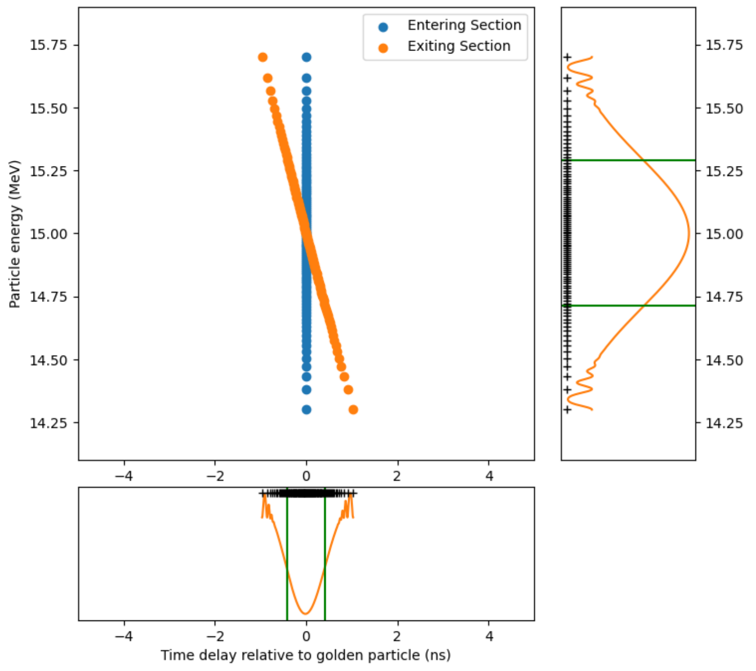

4 MeV/u Carbons

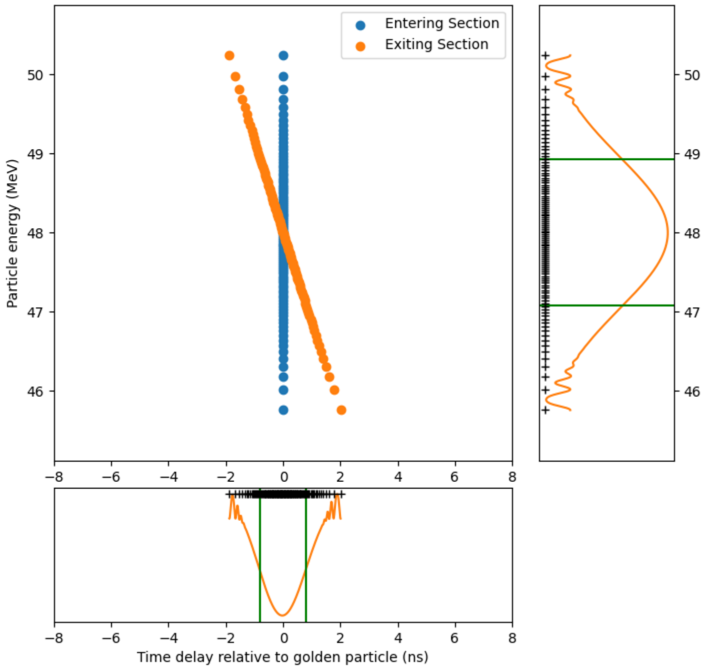

Energy: 48 ± 0.92 MeV (1.92%)
Bunch Length: 1.60 ns

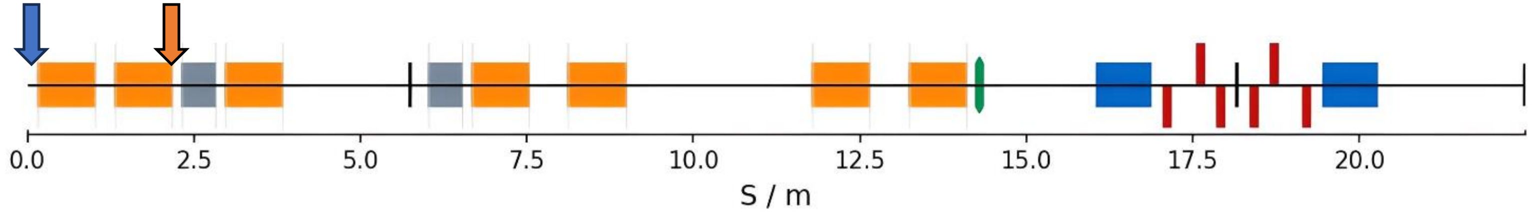

Longitudinal Phase Space Simulation – Cavities OFF

Energy: 15 ± 0.29 MeV (1.92%)
Bunch Length: 1.00 ns

15 MeV Protons

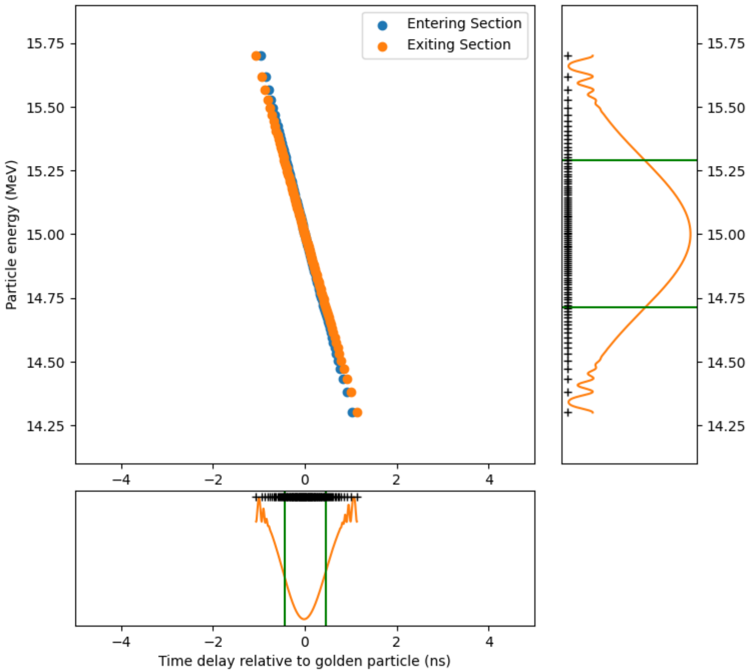

4 MeV/u Carbons

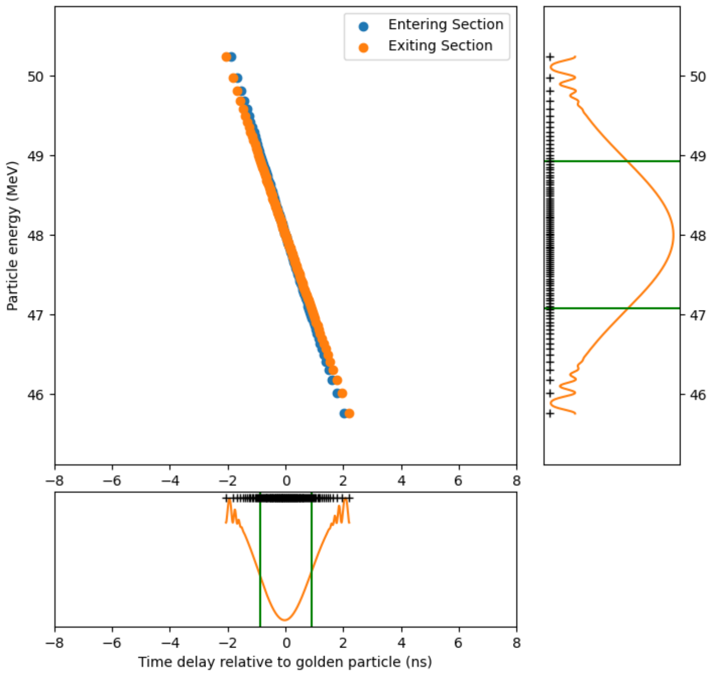

Energy: 48 ± 0.92 MeV (1.92%)
Bunch Length: 1.94 ns

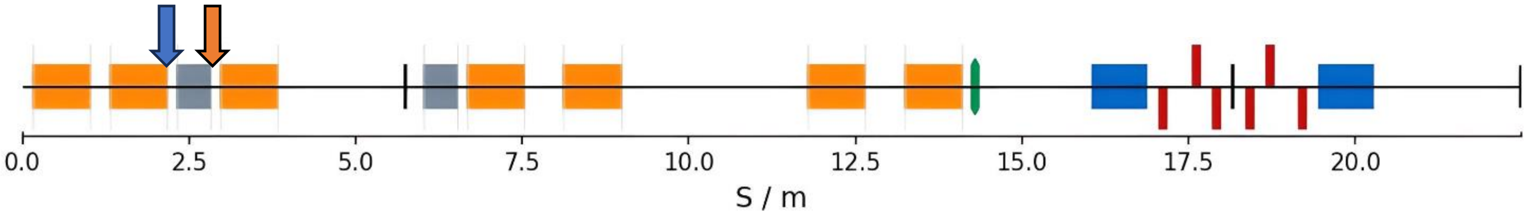

RF Cavities

Longitudinal Phase Space Simulation – Cavities OFF

Energy: 15 ± 0.29 MeV (1.92%)
Bunch Length: 2.14 ns

15 MeV Protons

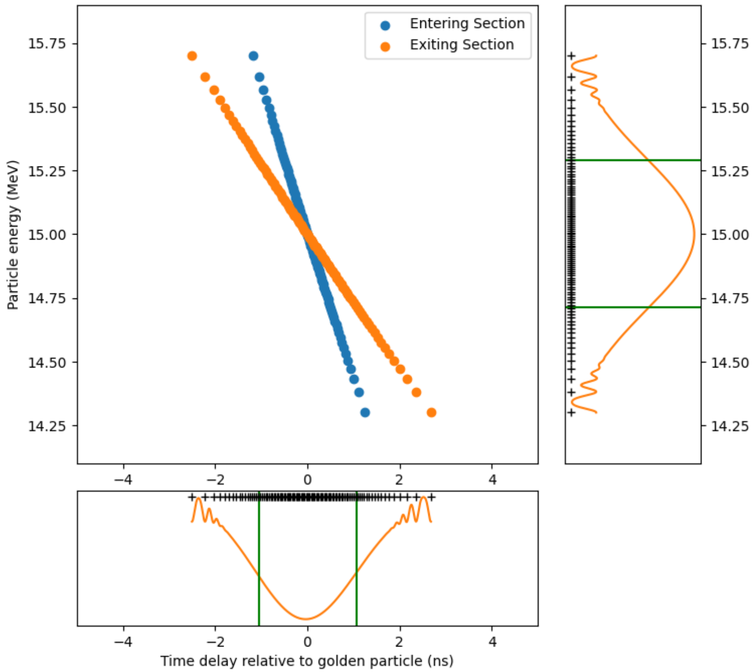

4 MeV/u Carbons

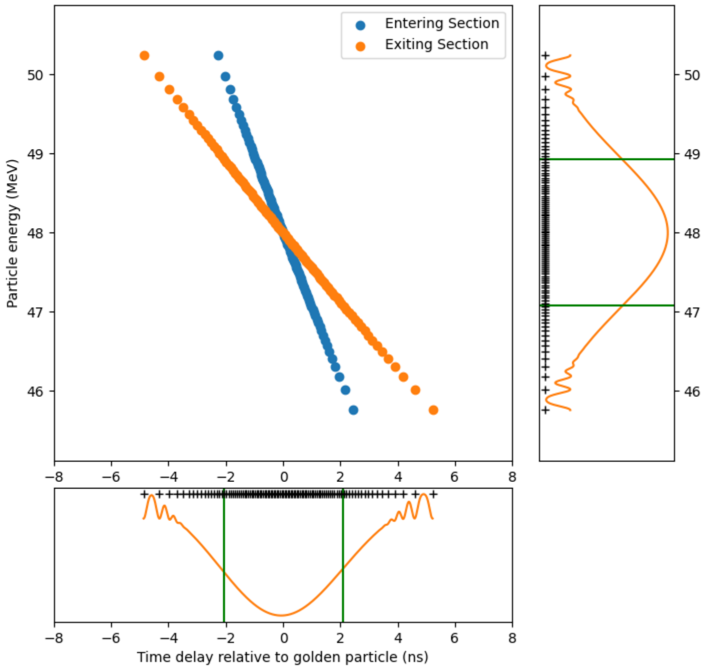

Energy: 48 ± 0.92 MeV (1.92%)
Bunch Length: 4.16 ns

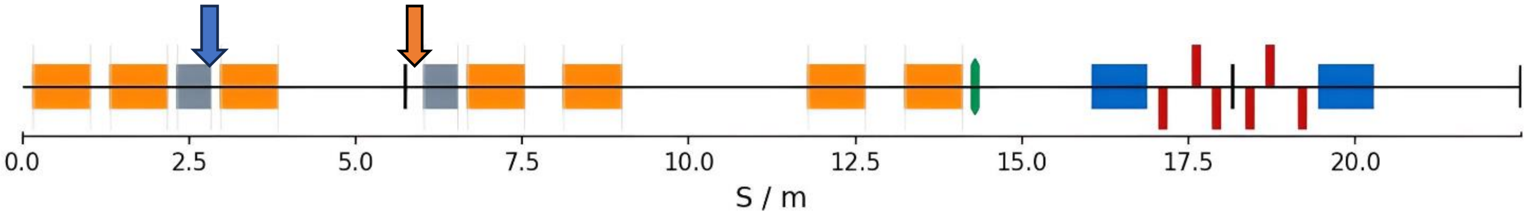

RF Cavities

Longitudinal Phase Space Simulation – Cavities OFF

Energy: 15 ± 0.29 MeV (1.92%)
Bunch Length: 2.32 ns

15 MeV Protons

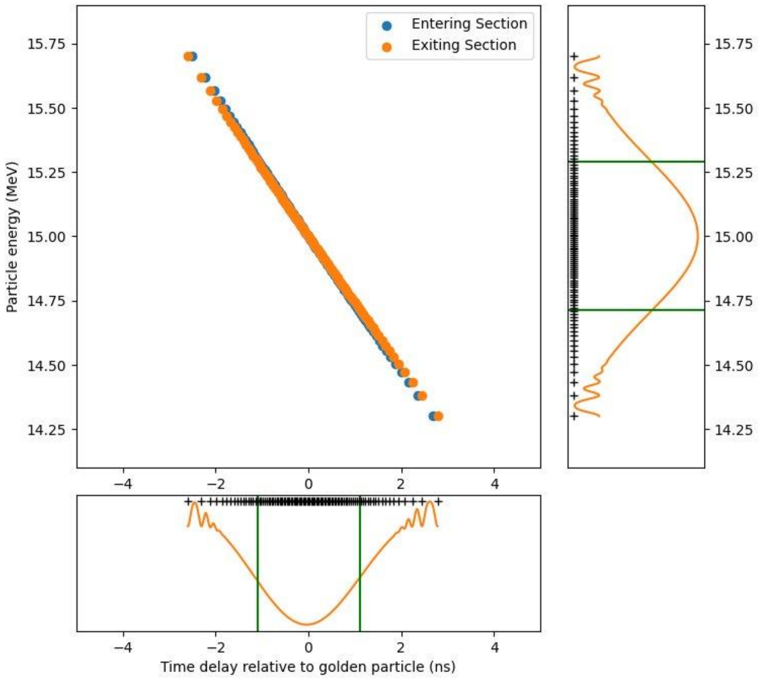

4 MeV/u Carbons

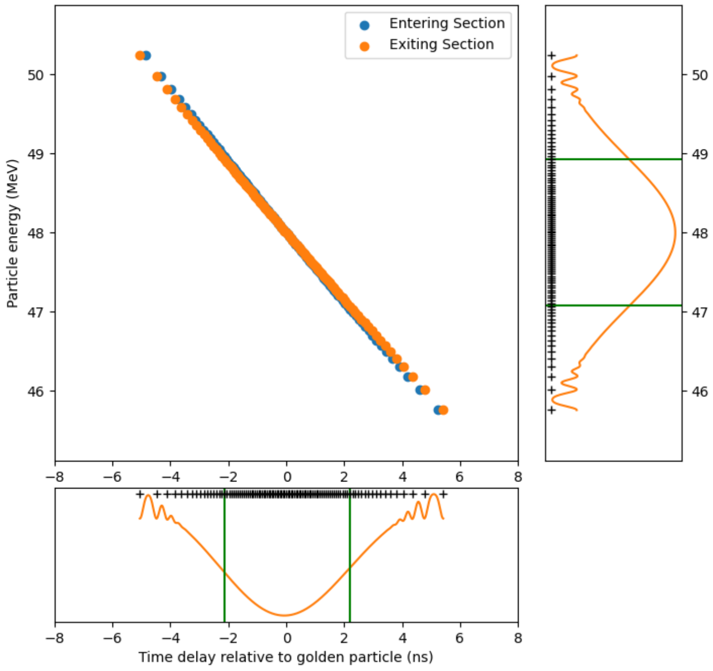

Energy: 48 ± 0.92 MeV (1.92%)
Bunch Length: 4.50 ns

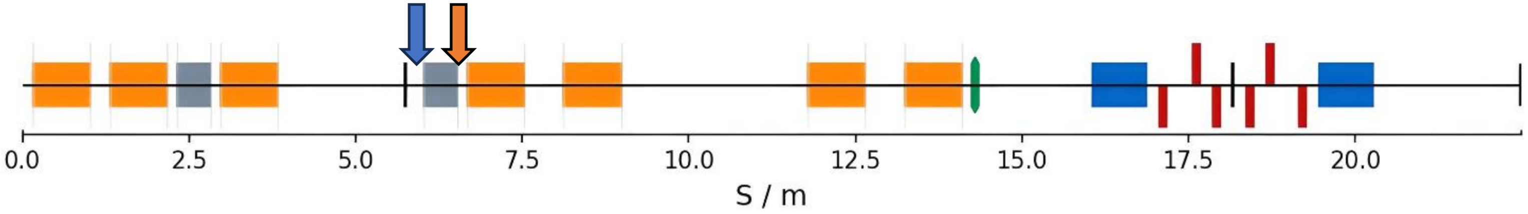

RF Cavities

Longitudinal Phase Space Simulation – Cavities OFF

Energy: 15 ± 0.29 MeV (1.92%)
Bunch Length: 4.00 ns

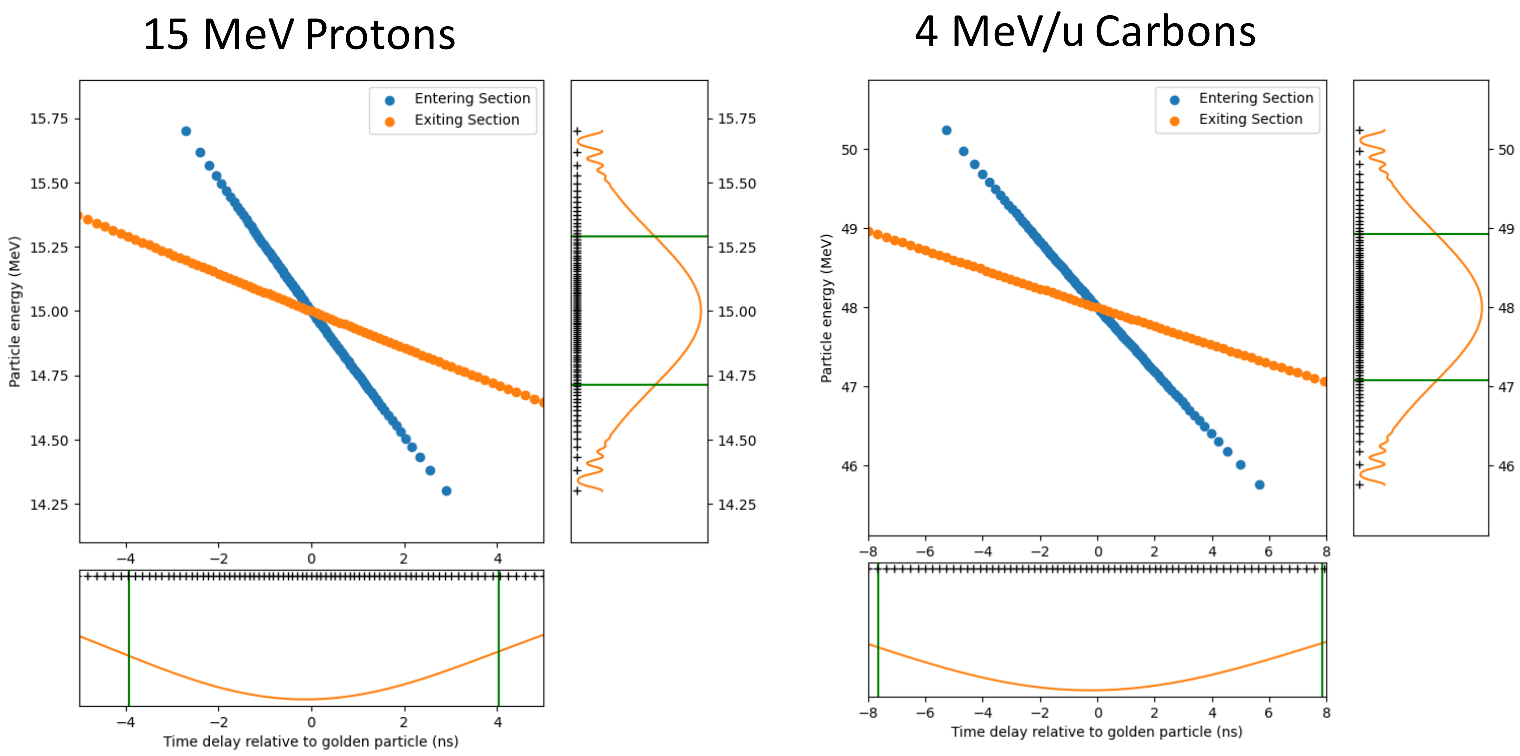

Energy: 48 ± 0.92 MeV (1.92%)
Bunch Length: 15.50 ns

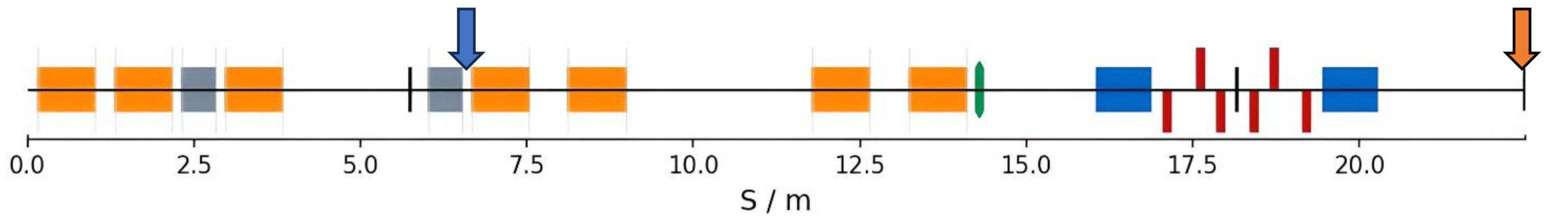

RF Cavities

Longitudinal Phase Space Simulation – Cavities ON

15 MeV Protons

Energy: 15 ± 0.29 MeV (1.92%)
Bunch Length: 0.82 ns

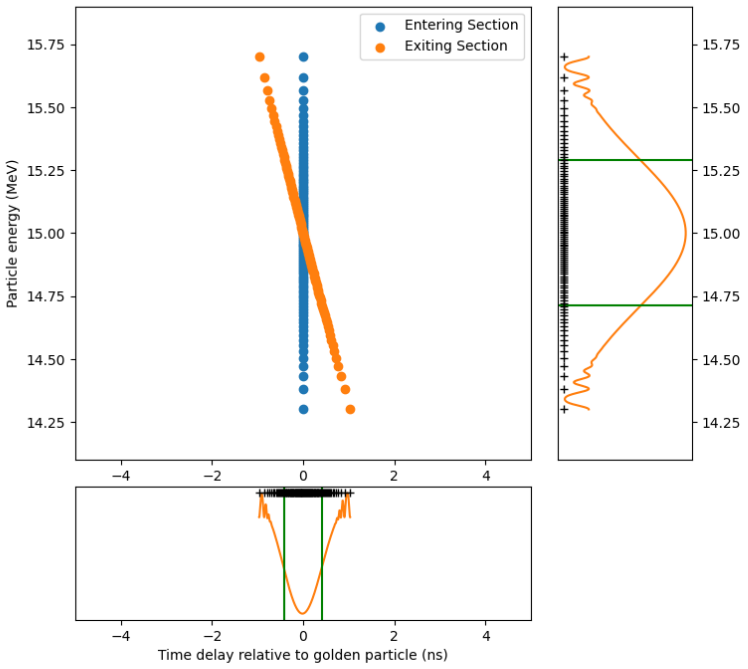

4 MeV/u Carbons

Energy: 48 ± 0.92 MeV (1.92%)
Bunch Length: 1.60 ns

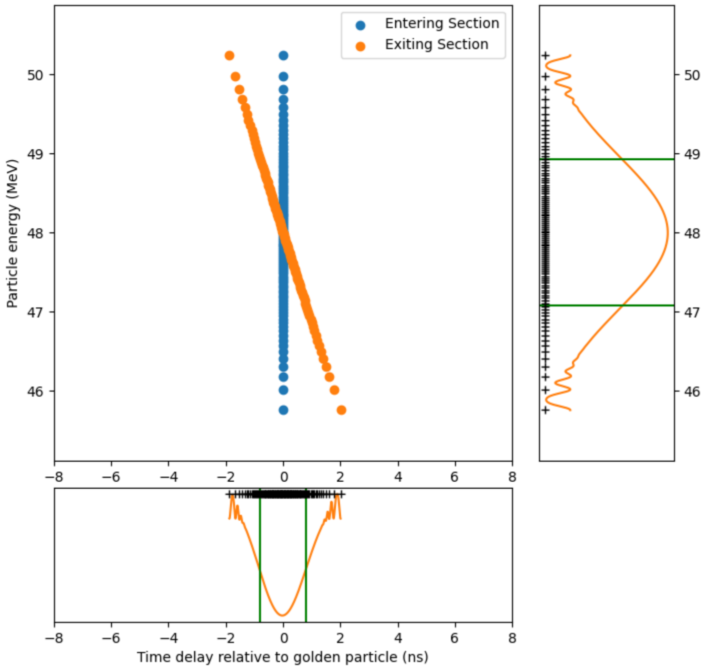

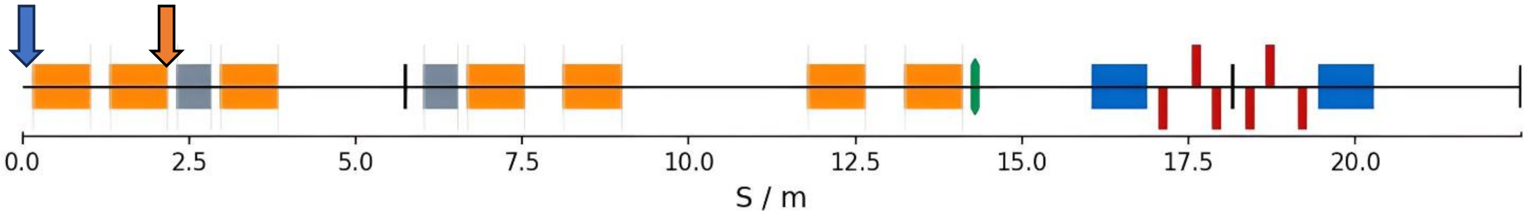

RF Cavities

Longitudinal Phase Space Simulation – Cavities ON

15 MeV Protons

Energy: 15 ± 0.09 MeV (0.61%)
Bunch Length: 0.90 ns

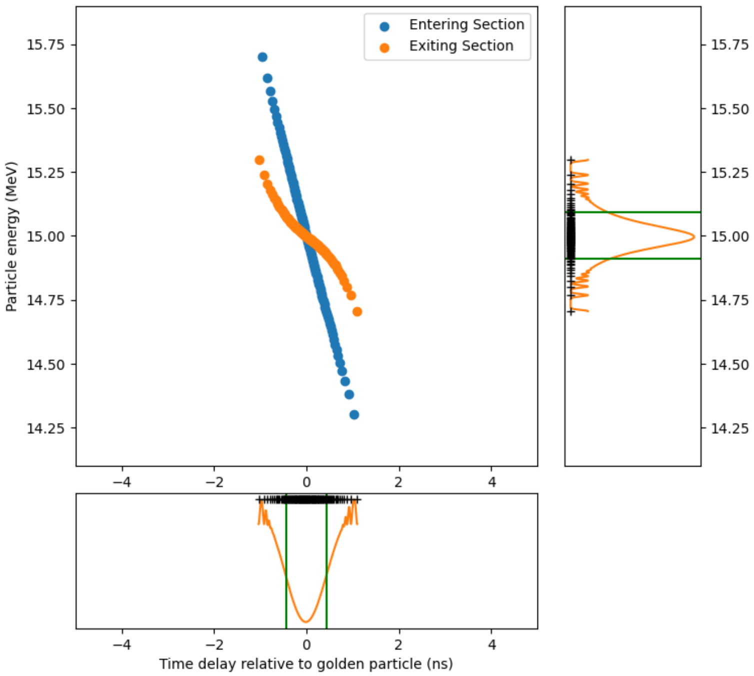

4 MeV/u Carbons

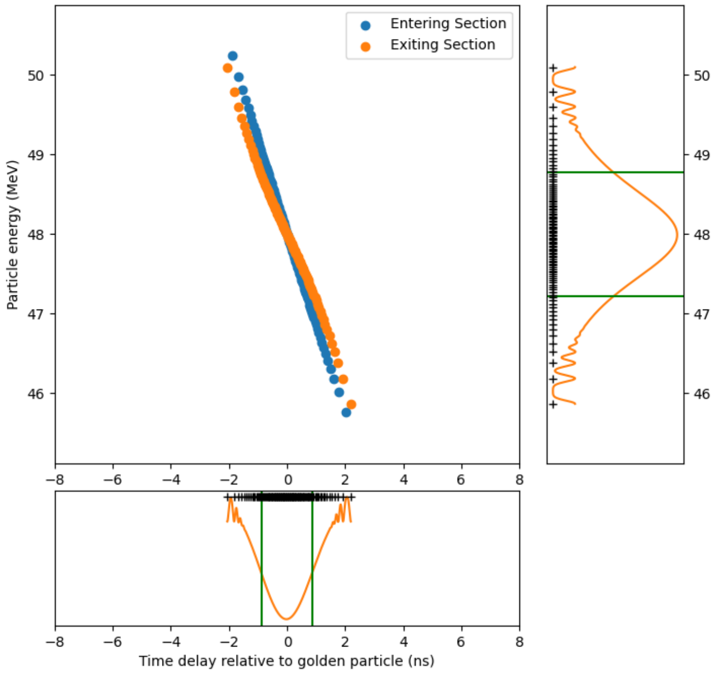

Energy: 48 ± 0.78 MeV (1.62%)
Bunch Length: 1.90 ns

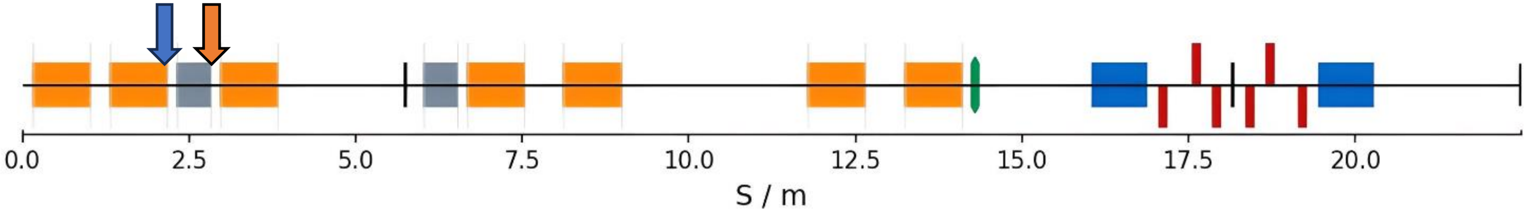

Longitudinal Phase Space Simulation – Cavities ON

Energy: 15 ± 0.09 MeV (0.61%)
Bunch Length: 1.26 ns

15 MeV Protons

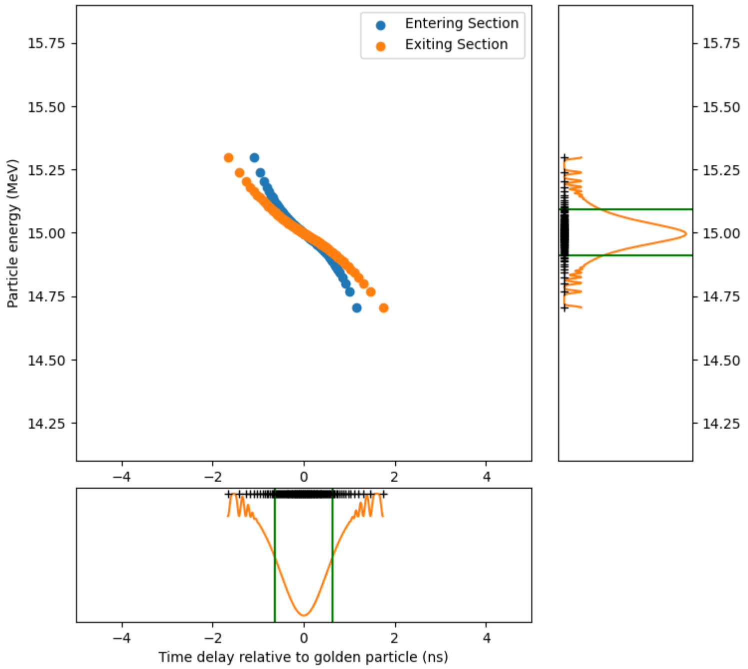

4 MeV/u Carbons

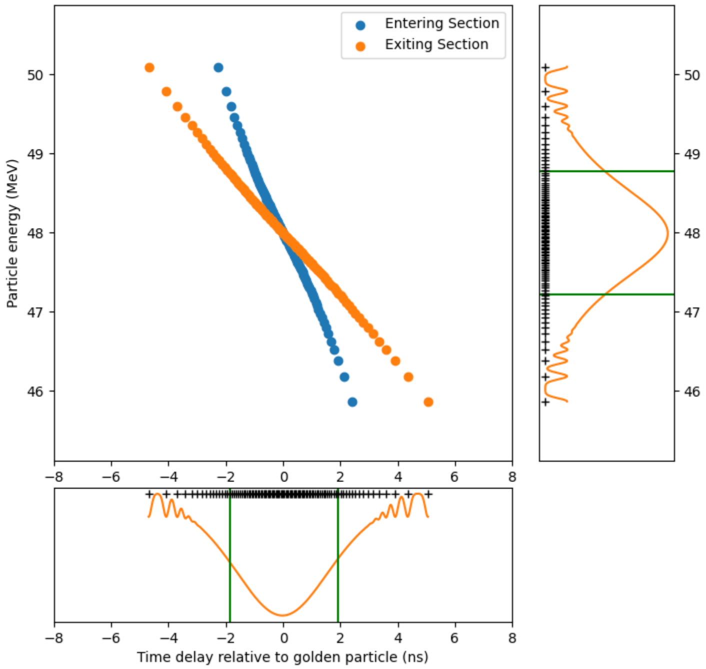

Energy: 48 ± 0.92 MeV (1.62%)
Bunch Length: 3.76 ns

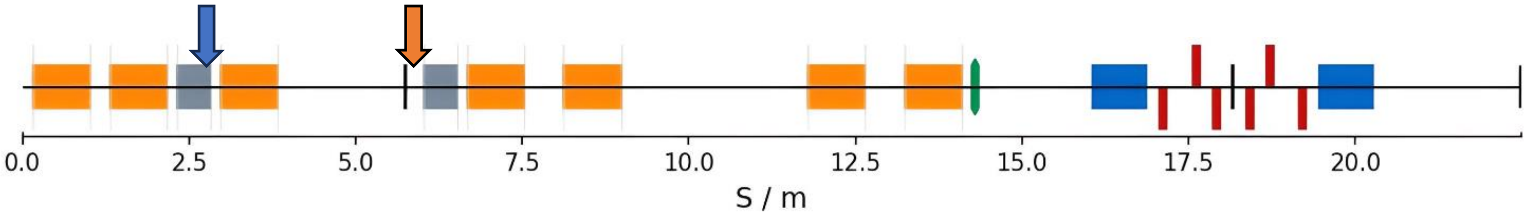

RF Cavities

Longitudinal Phase Space Simulation – Cavities ON

Energy: 15 ± 0.05 MeV (0.31%)
Bunch Length: 1.26 ns

Operating at 45% of Design E-field

15 MeV Protons

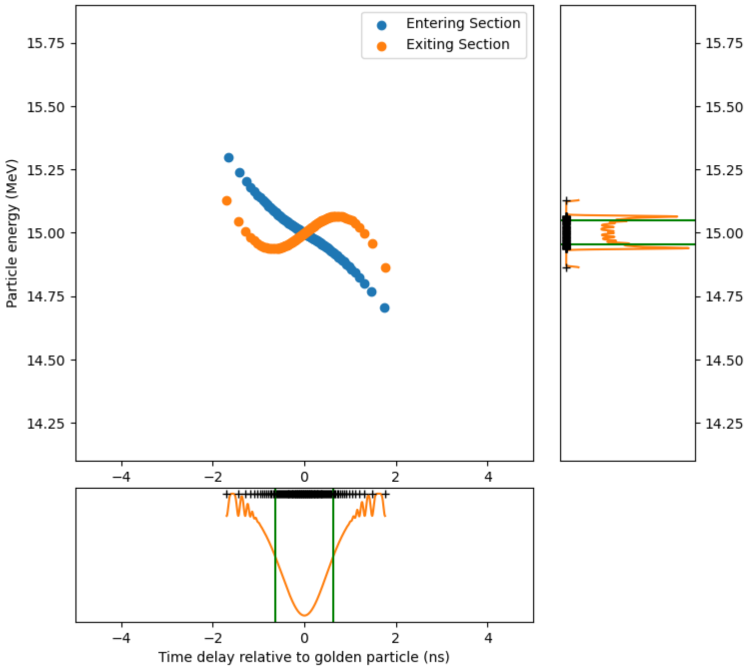

4 MeV/u Carbons

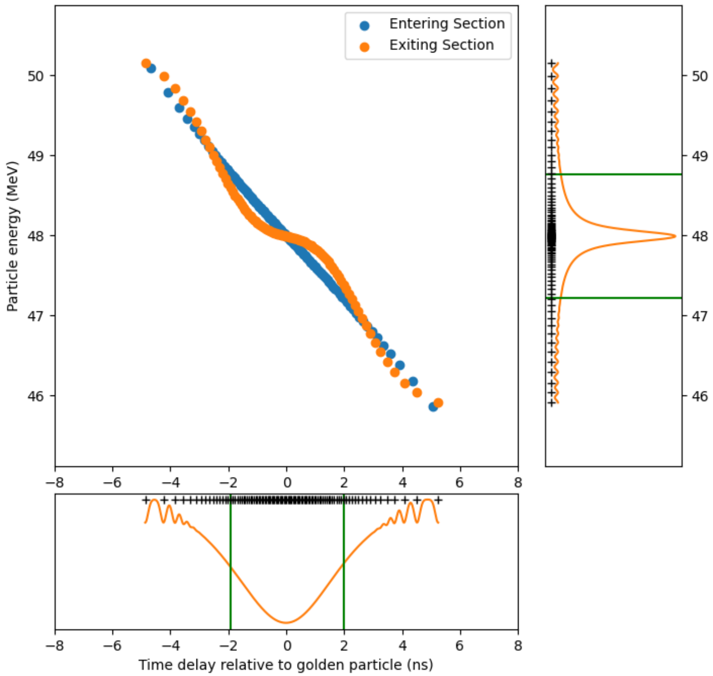

Energy: 48 ± 0.77 MeV (1.61%)
Bunch Length: 4.04 ns

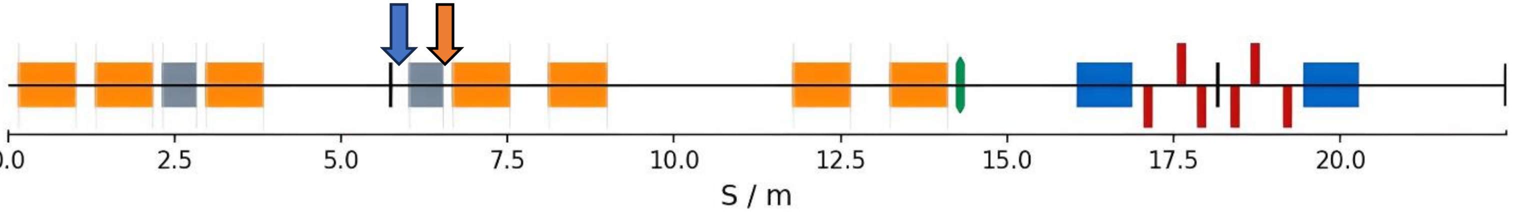

RF Cavities

Longitudinal Phase Space Simulation – Cavities ON

15 MeV Protons

Energy: 15 ± 0.05 MeV (0.31%)
Bunch Length: 1.18 ns

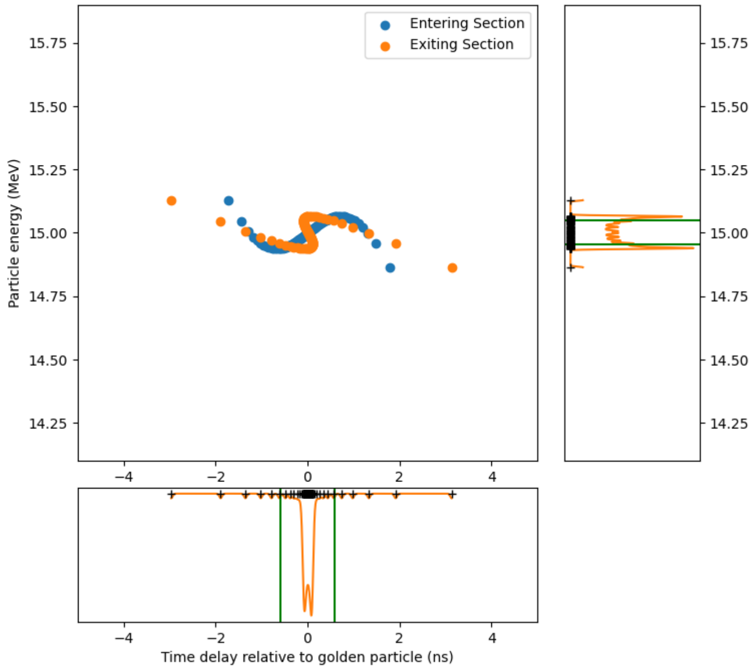

4 MeV/u Carbons

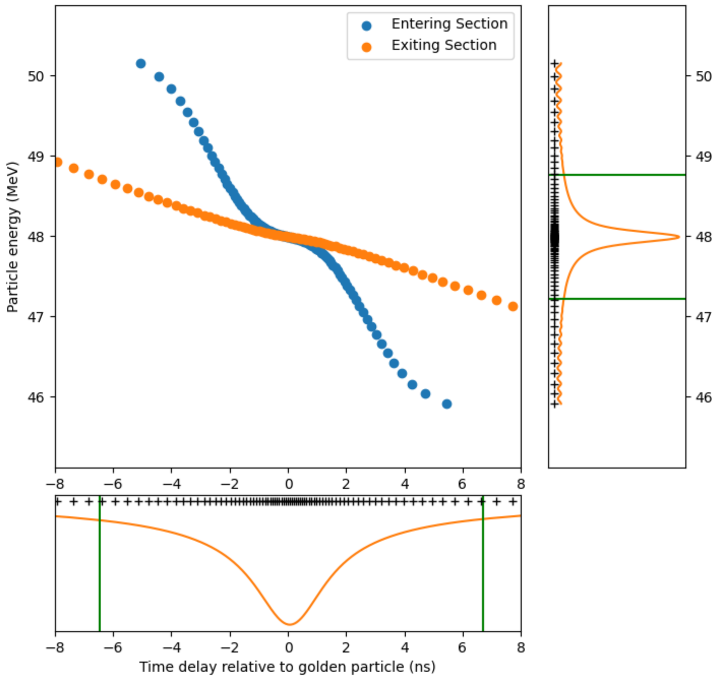

Energy: 48 ± 0.77 MeV (1.61%
Bunch Length: 13.16 ns

Highly non-gaussian bunch shapes not described well b standard deviation metric

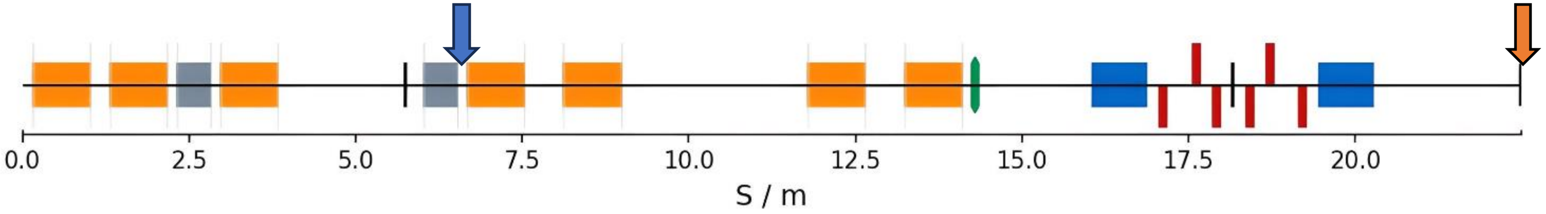

RF Cavities

John Adams Institute for Accelerator Science

Longitudinal Phase Space Simulation – Results

15 MeV Protons

OFF

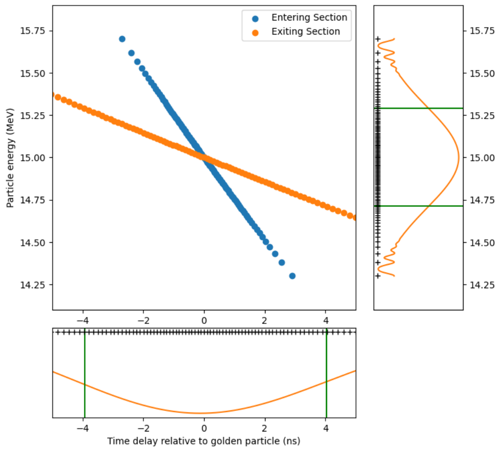

ON

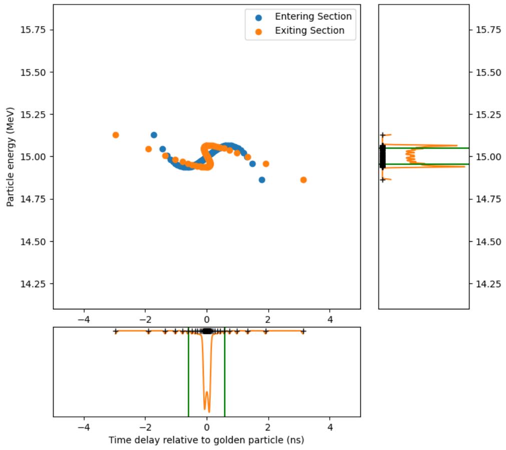

Bunch Length	Energy Spread
4.00 ns	1.92%
↓	↓
1.18 ns	0.31%

4 MeV/u Carbons

OFF

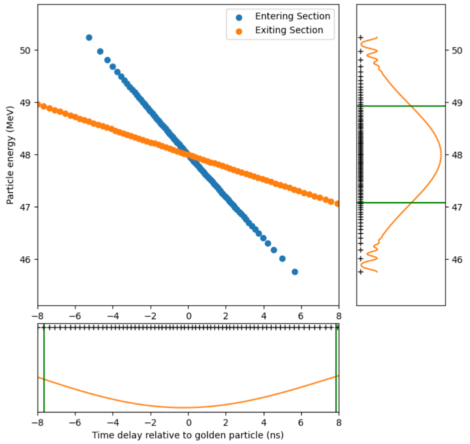

ON

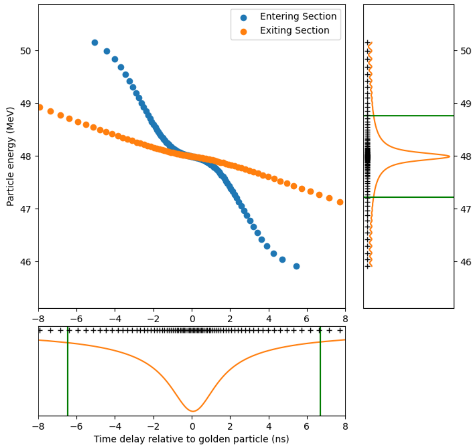

Bunch Length	Energy Spread
15.50 ns	1.92%
↓	↓
13.16 ns	1.61%

RF Cavities

Final Cavity Geometry

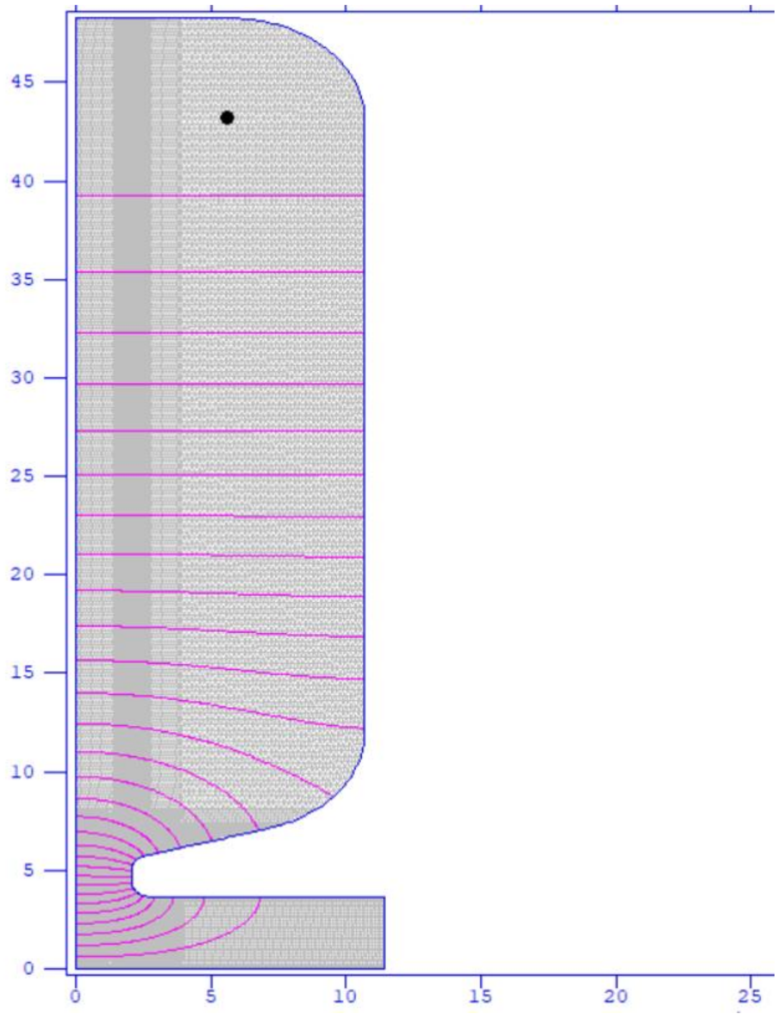

Parameter	Value
Frequency [MHz]	201
Shunt Impedance - Z [MOhm/m]	25.41
Transit time factor -T []	0.33
ZTT [MOhm/m]	2.91
Maximum E field [MV/m] @ kilpatrick – 1.5	22.15
Maximum E field on axis [MV/m] @ kilpatrick – 1.5	8.08

3D Simulation with CST

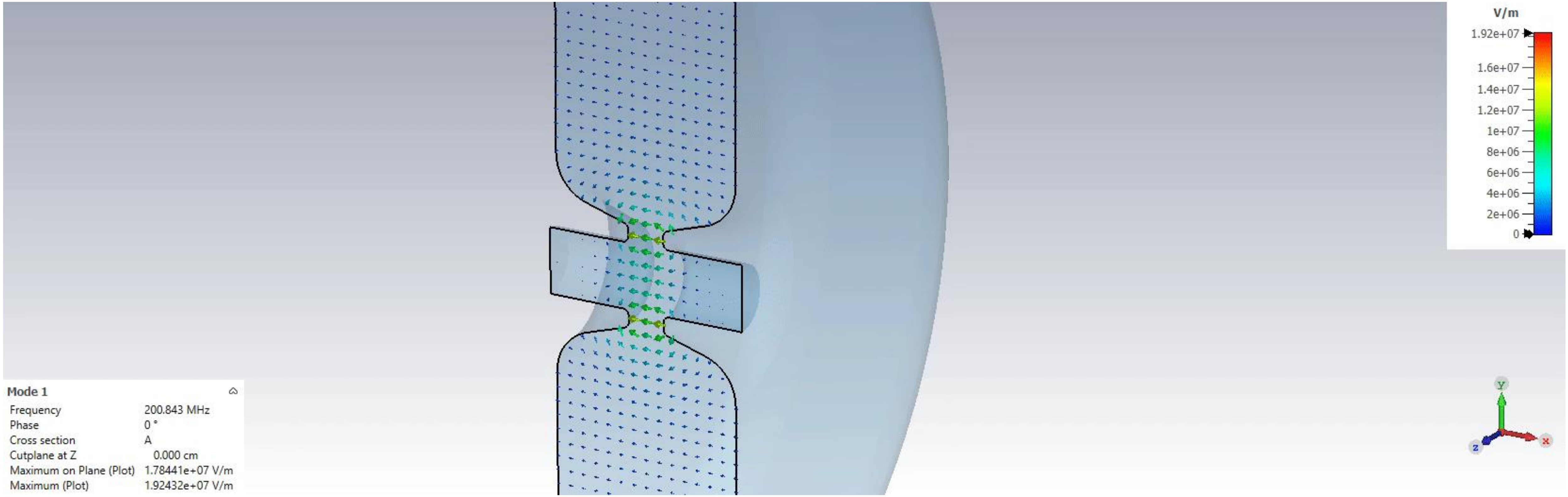

SuperFish vs CST

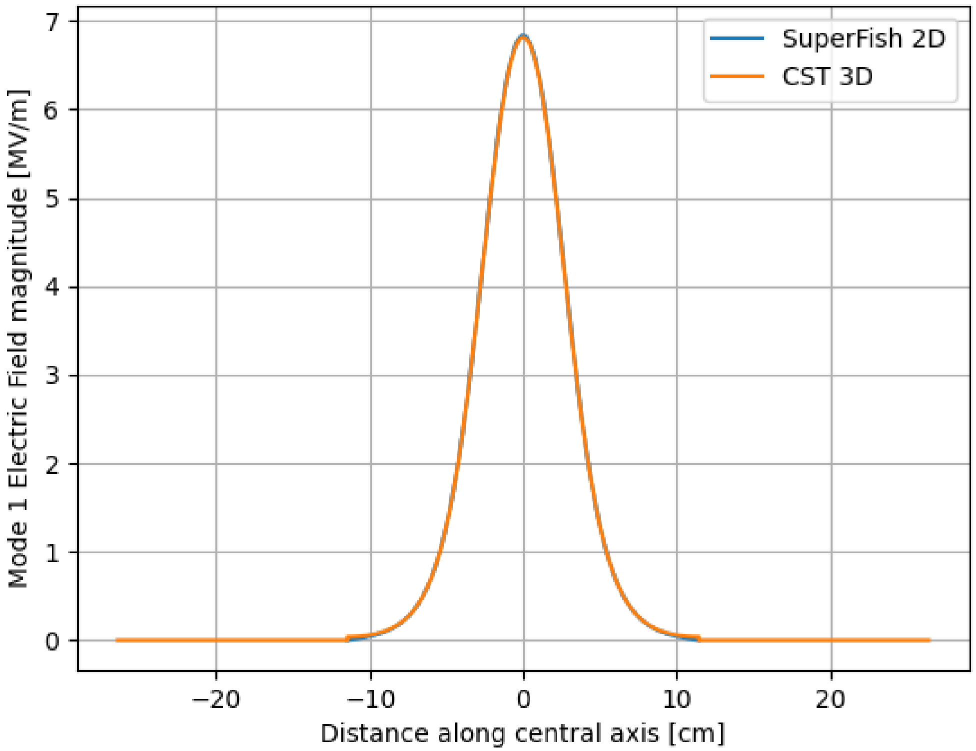

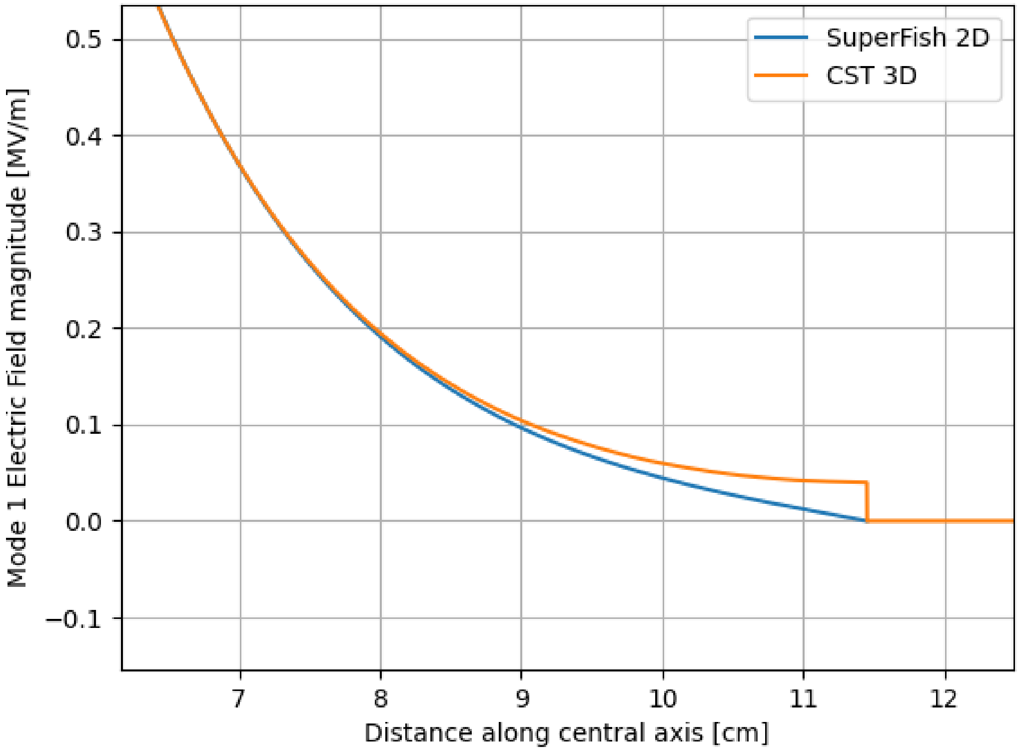

- Scaled by the stored energy in the cavity.
- Size of the electric field is somewhat arbitrary. We are looking a relative differences here.

Simulation of the 3D Field Map in the BDSIM Lattice

- Simulation in BDSIM using the 3D field map from CST.
- Validated the cavity design and shown good control of the longitudinal phase space
- Final energy spread 0.68%

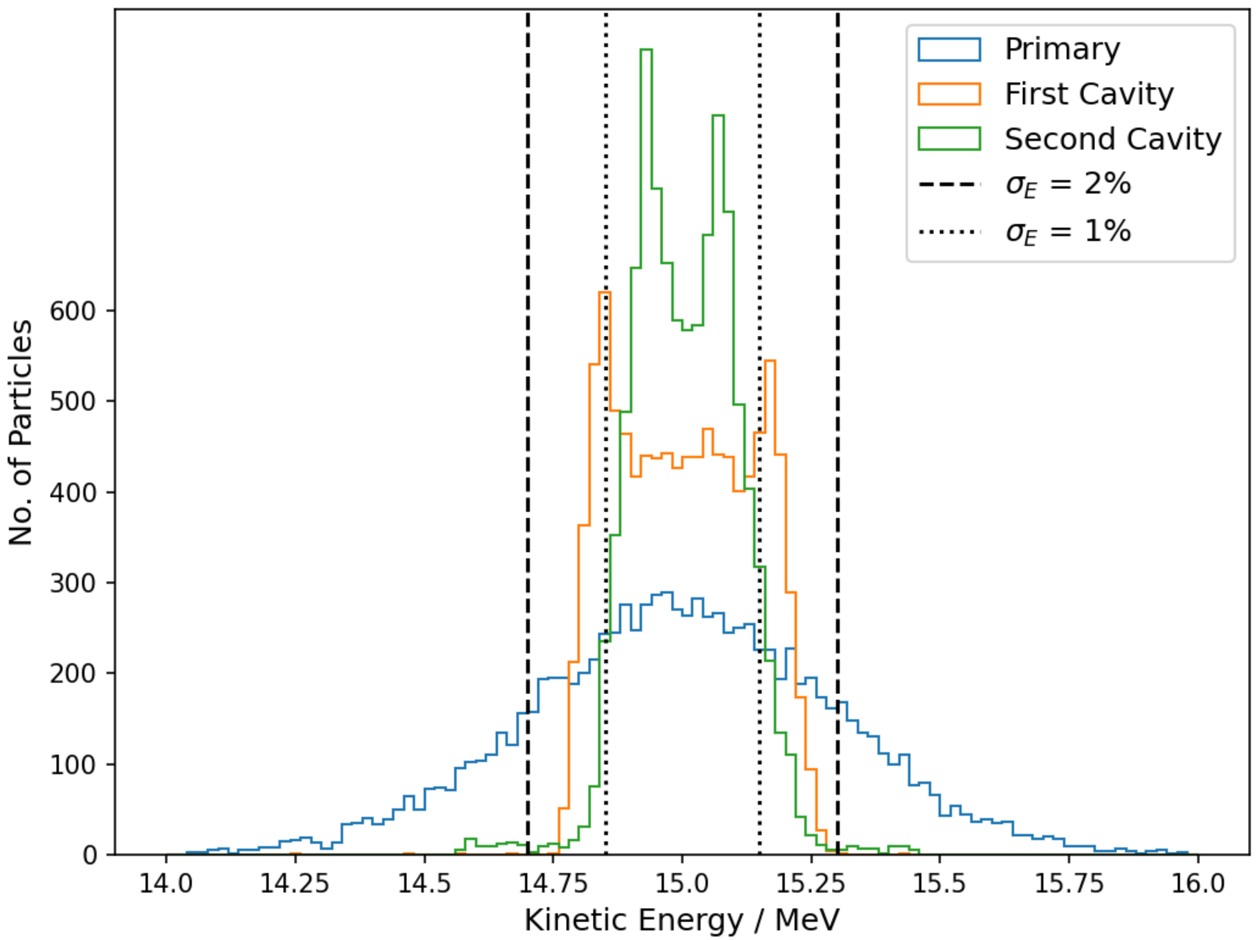

Comparison of Longitudinal Phase-space Simulations

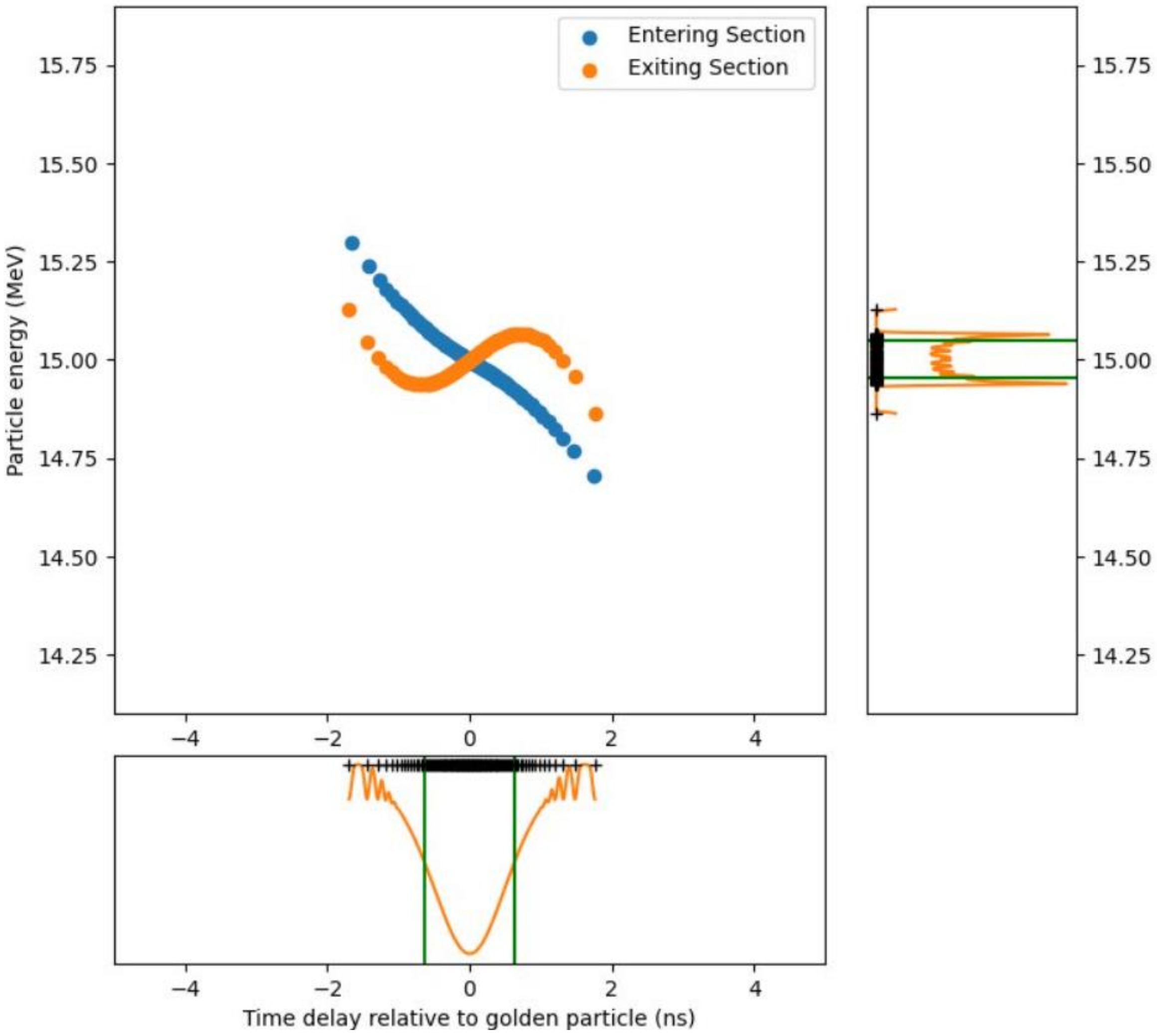

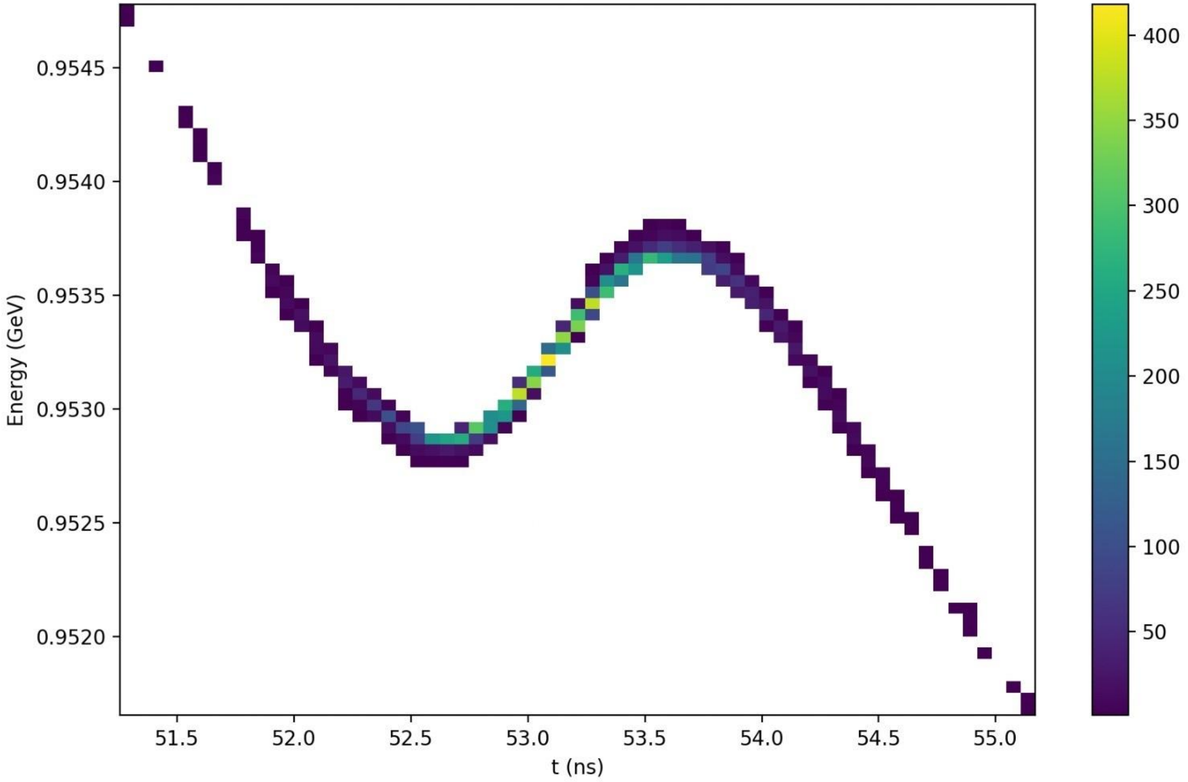

RF Cavities

RF Cavities Summary

- Designed & optimised a 3D cavity design for LhARA stage 1.
- Validated the design with 6D tracking in BDSIM.

Future work:

- Investigate schemes to better control the carbon beam.
- Continue design is CST, waveguides and waveguide ports.
- Continue optimisation using BDSIM.
- Additional RF infrastructure, cavity phasing.

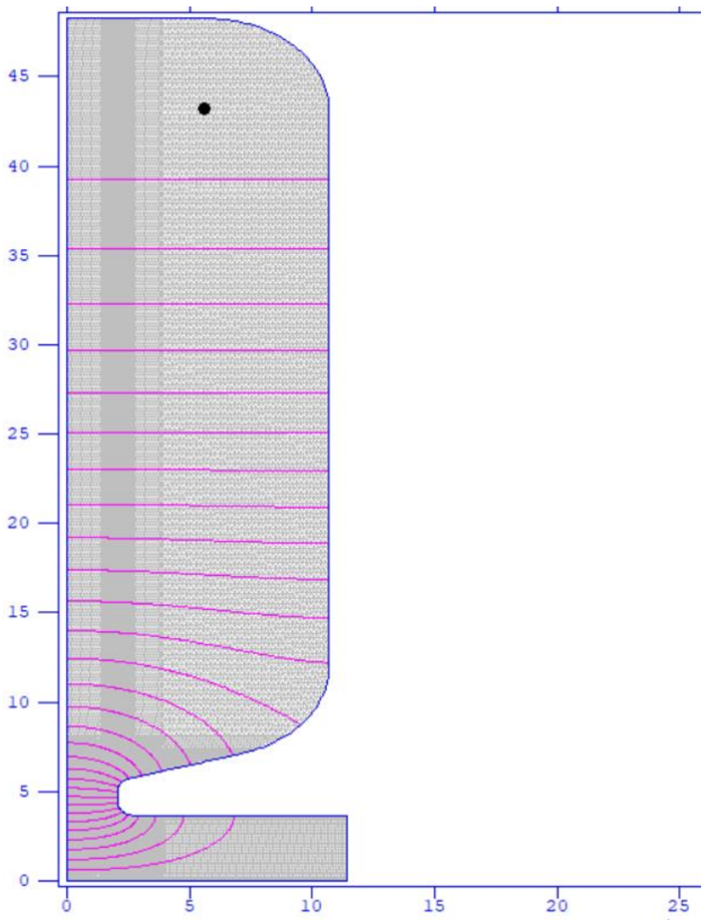

Magnet Design

Sam Leadley (samuel.leadley@physics.ox.ac.uk)
University of Oxford
Carl Jolly (carl.jolly@physics.ox.ac.uk)
University of Oxford

Magnet Design

Beam Parameters	
Energy	15 MeV
Momentum	0.168 GeV/c
Rigidity	0.561 Tm
Diameter	7.5 mm (1σ radius)

Magnet materials:
- Pure ***iron*** yokes
- ***Copper*** coils
- Vacuum/Air gaps

Good Field Region: 35mm (5σ radius)
Beam pipe radius: 50mm

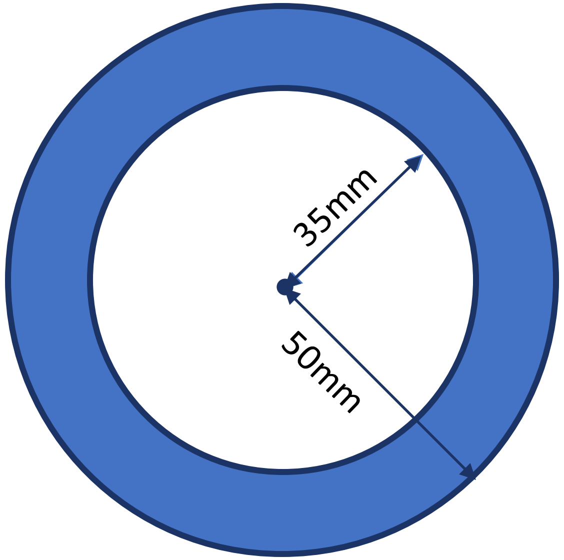

Required Magnets:

Vertical Arc Dipole:
Bending/beam ***selection*** into vertical arc

Vertical Arc Quadrupole:
Twiss manipulation and ***focusing*** in vertical arc

Extraction Octupole:
Flat beam profile

Nozzle Quadrupole:
Permanent magnet capturing beam after laser source

Magnetic Field Analysis

Polynomial Fit

$$B_y = \sum_{n=1}^{\infty} C_n x^{n-1}$$

Fit a curve to the absolute B-field value on a ***radial contour*** from the beamline to the edge of the beampipe.

Less accurate

- Monomial functions are ***not orthogonal***
  - Fit depends on chosen monomials
    - Easy to ***overfit*** data

Fourier Analysis

$$C_n = \frac{1}{M r_0^{n-1}} \sum_{m=0}^{M-1} B_m e^{-2\pi i n m / M}$$

Fourier transform of the B-field vector along an ***azimuthal contour*** around the Good Field Region of the beampipe.

More accurate

- Fourier coefficients are ***orthogonal***
  - Fit is always the same
- Compare ***normal & skew*** components

Switching Dipole

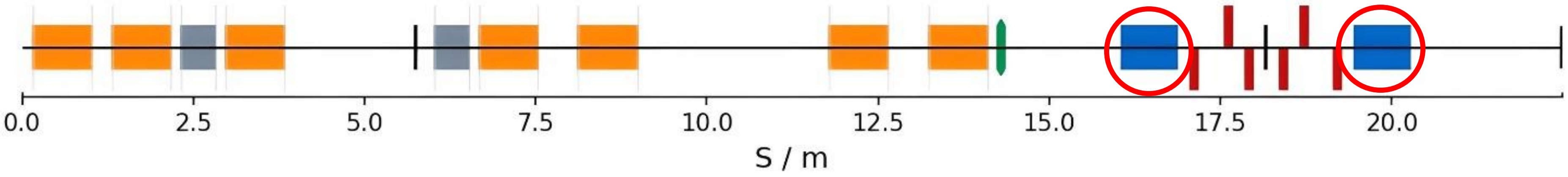

Initial requirements:

- $B_{gap} = 0.551$ T
- $B_{yoke} \leq 2.0$ T
- GFR field purity ≥ 99.9%

Coil Parameters	
Coil Area	20,000 mm^2
Current Density	0.93 Amm^{-2}
Turns	50
Cooling Method	Radiative

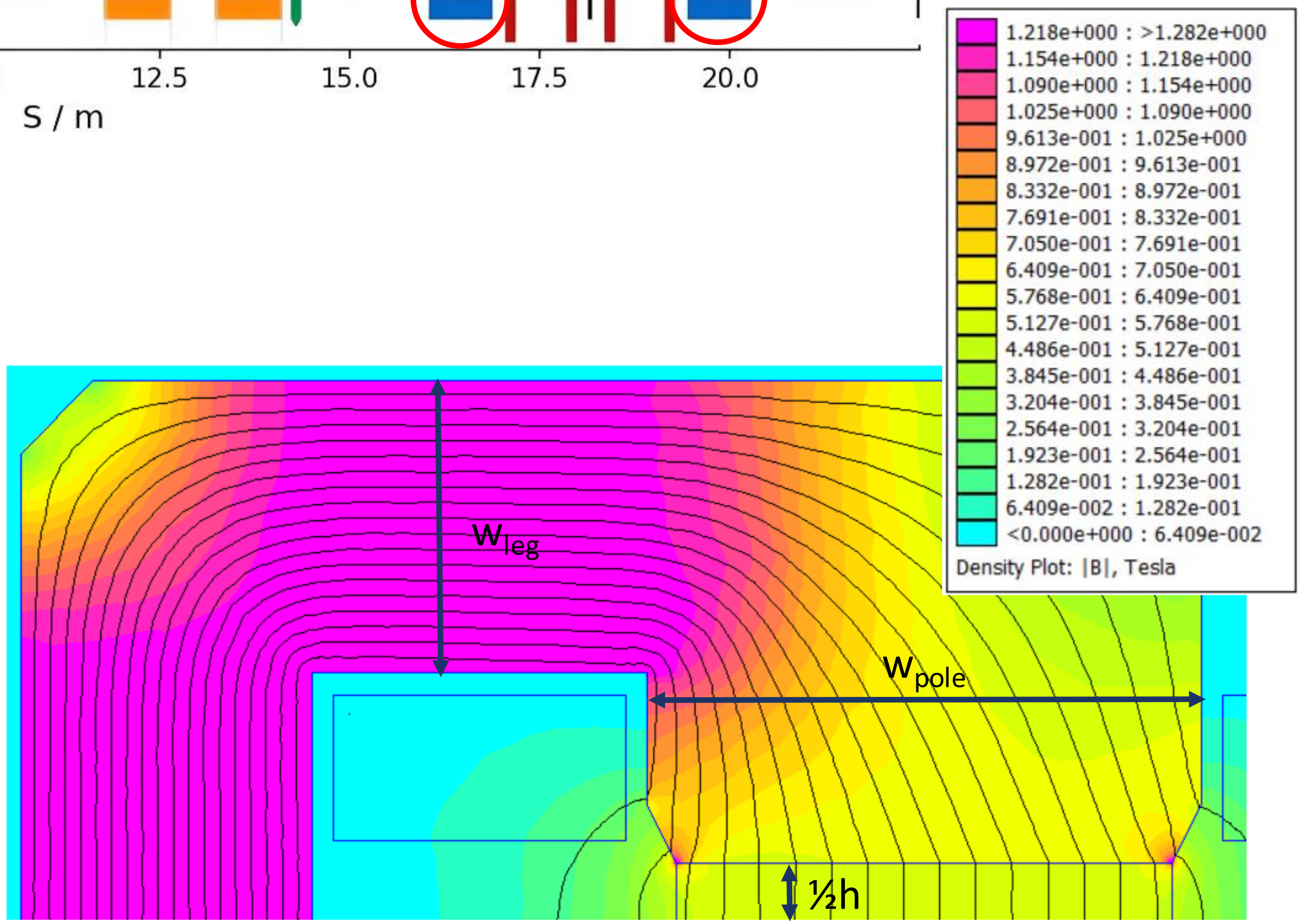

FEMM 4.2 output of ½-dipole magnet B-field, mesh size 0.03mm. C-shape for easy beam switching.

Magnet Design

Dipole GFR Field

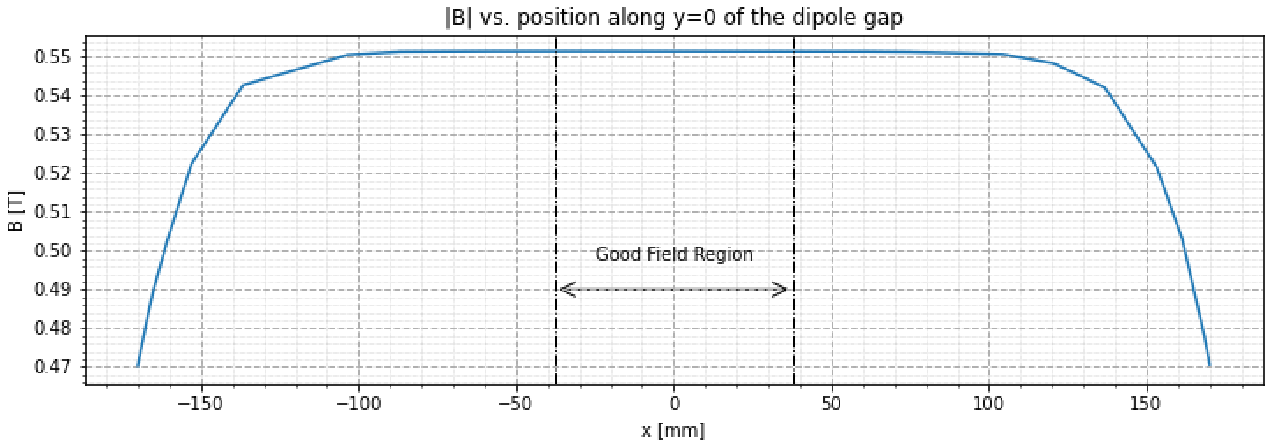

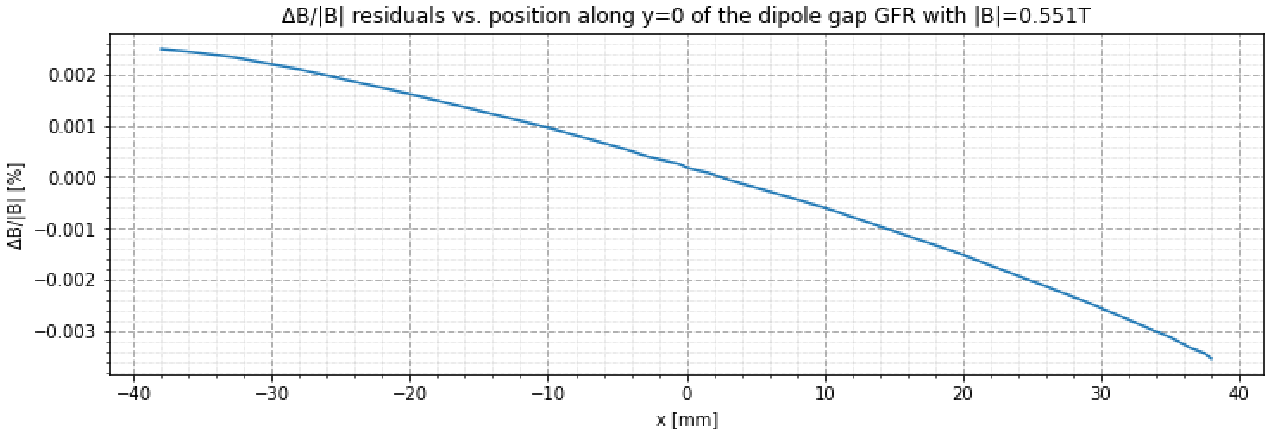

Simple fit takes **average B** across the **GFR** to assign a value to the field.

Standard dipole equations:

- $w_{pole}=w_{GFR}+2.5h$
- $B_{leg}=B_{gap}*(w_{pole}+1.2h)/w_{leg}$

Magnet Design

Dipole Field Analysis

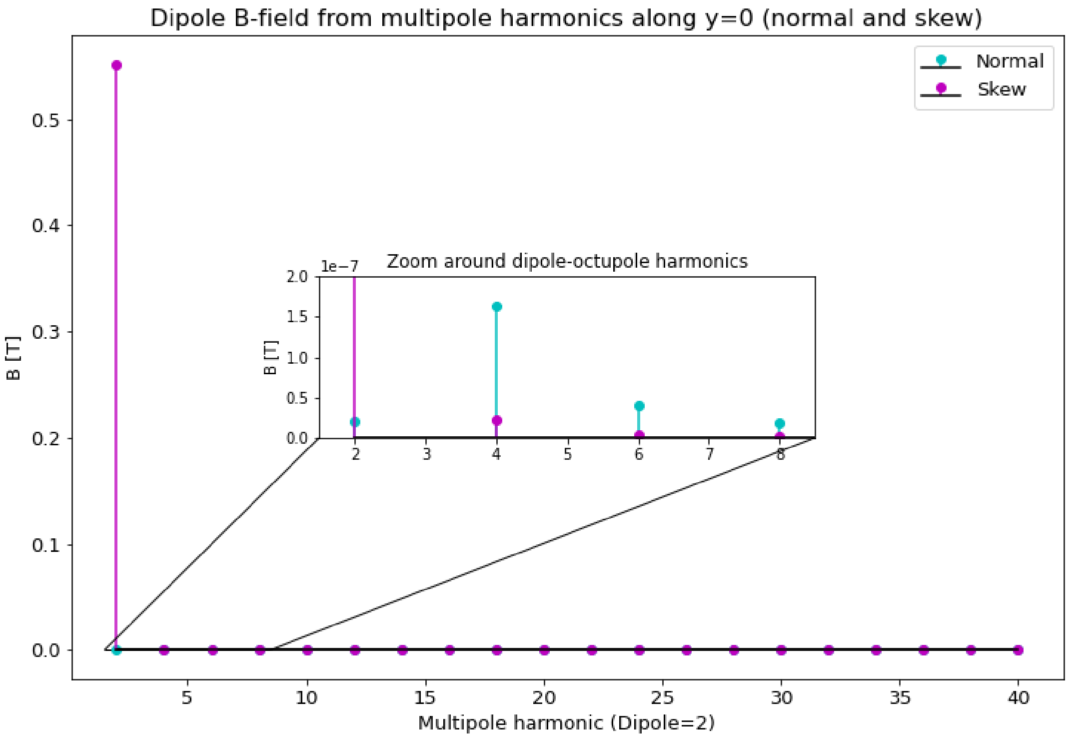

Harmonic	K-value (normal)	K-value (skew)	B@R=R_{GFR}
Dipole	**0.0 m^{-1}**	**0.551 m^{-1}**	**0.551 T**
Quadrupole	1.0×10^{-5} m^{-2}	*0.0 m^{-2}*	0.160 μT
Sextupole	1.2×10^{-4} m^{-3}	*1.0×10^{-5} m^{-3}*	0.041 μT
Octupole	4.5×10^{-3} m^{-4}	*2.9×10^{-4} m^{-4}*	0.018 μT
Decapole	0.291 m^{-5}	*0.0146 m^{-5}*	0.010 μT
Dodecapole	26.582 m^{-6}	*1.065 m^{-6}*	0.007 μT
14-pole (k6)	3165.3 m^{-7}	*107.93 m^{-7}*	0.005 μT
16-pole (k7)	4.7×10^{5} m^{-8}	*1.3×10^{4} m^{-8}*	0.003 μT

N.B. all values given are positive, no distinction is given to ±k
Main k in red bold, allowed harmonics in red italics.

Vertical Arc Quadrupole

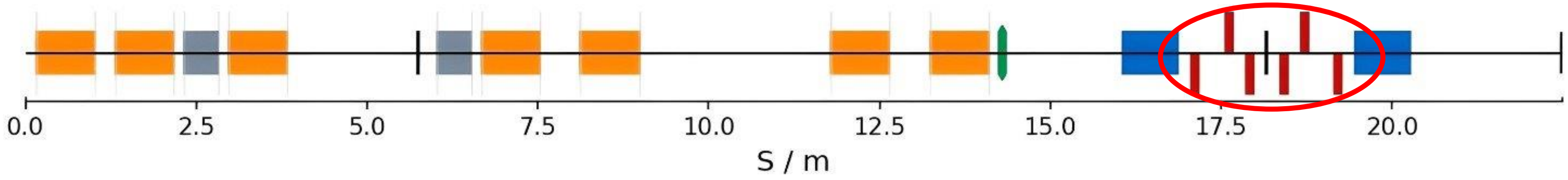

Initial requirements:

- $K_1 = 32.0\ m^{-2}$
- $B_{max} \leq 2.0$ T
- GFR field purity ≥ 99.9%

Coil Parameters	
Coil Area	4,070 mm^2
Current Density	5.31 Amm^{-2}
Turns	18
Cooling Method	Water cooled

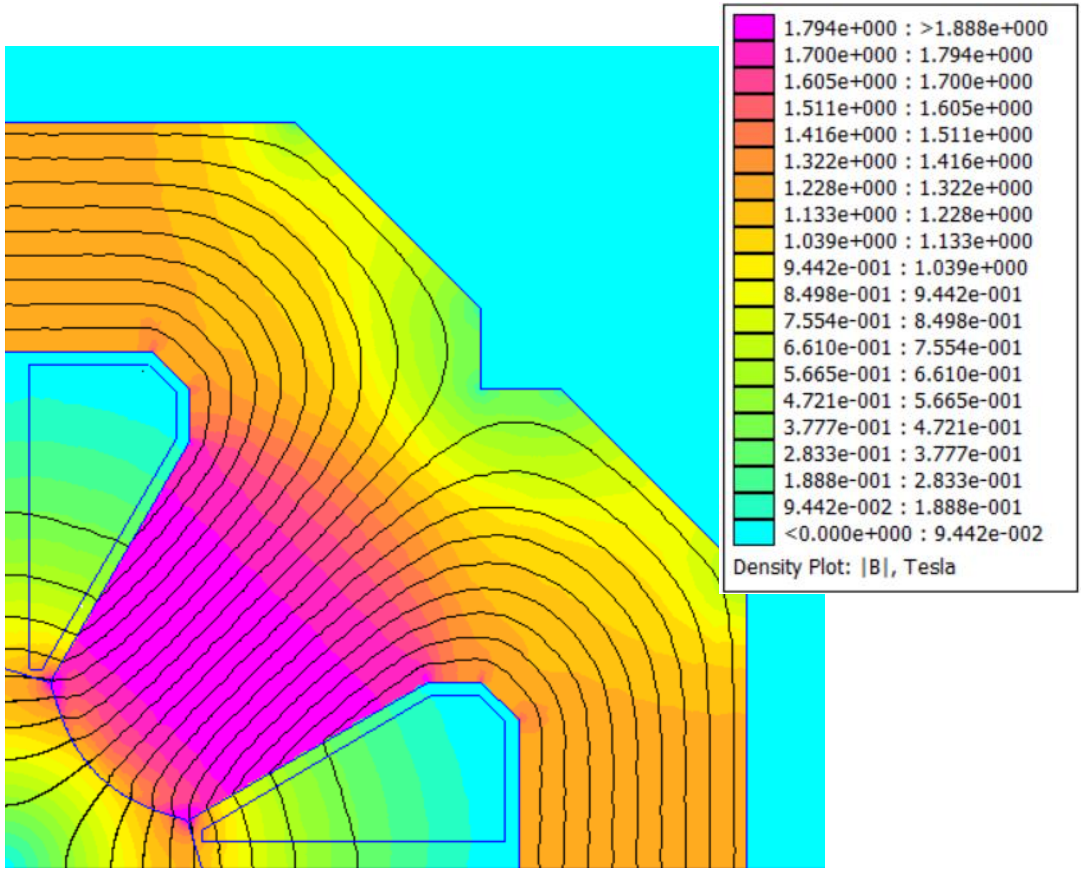

FEMM 4.2 output of ¼-quadrupole magnet B-field, mesh size 0.03mm

Quadrupole GFR Field

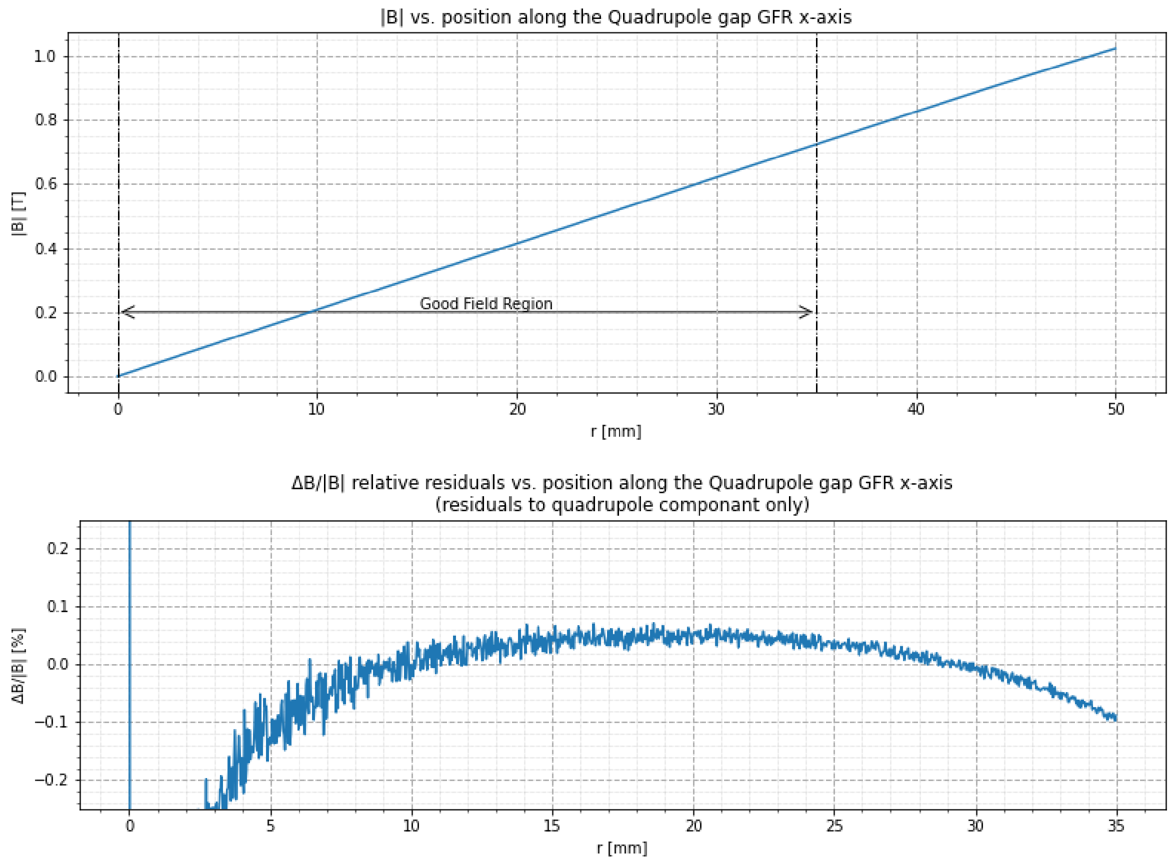

Quadrupole fitted with calculated $\mathbf{k_1 = 36.96m^{-2}}$

Residuals <0.1% for most of the GFR. Central part dominated by **mesh error** due to **small fields**

Quadrupole Field Analysis

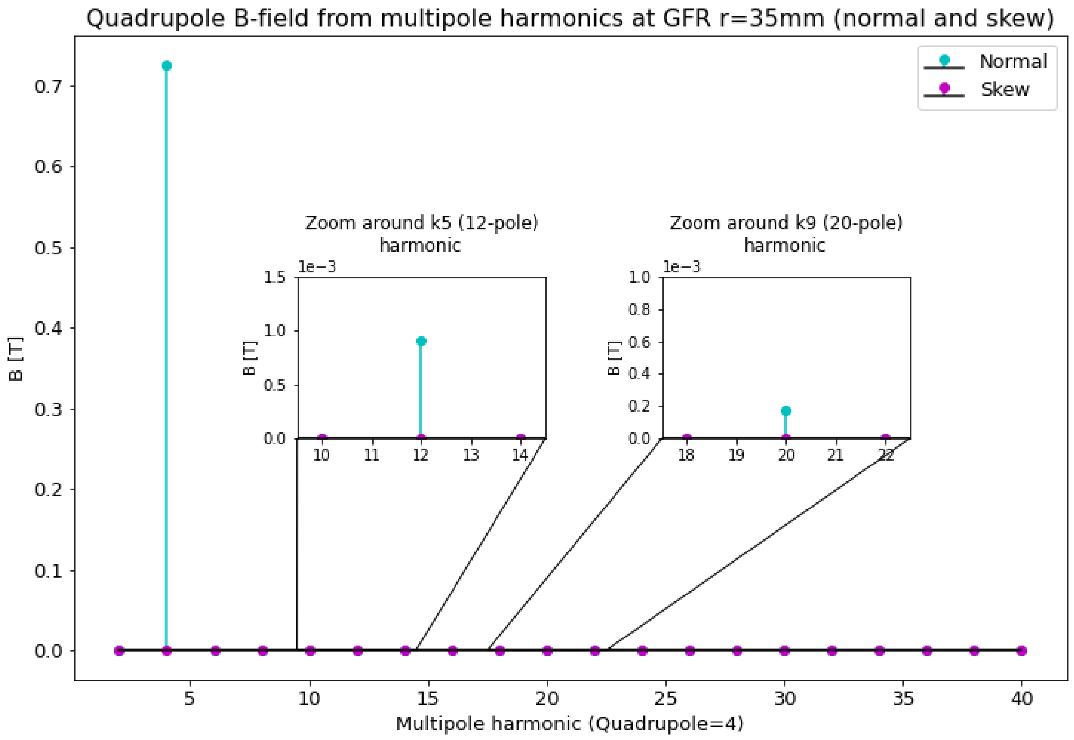

Harmonic	K-value (normal)	K-value (skew)	B@R=R_{GFR}
Dipole	0.0 m^{-1}	0.0 m^{-1}	0.0 T
Quadrupole	**36.958 m^{-2}**	**0.058 m^{-2}**	**0.726 T**
Sextupole	0.0 m^{-3}	0.0 m^{-3}	0.0 T
Octupole	0.0 m^{-4}	0.0 m^{-4}	0.0 T
Decapole	0.0 m^{-5}	0.0 m^{-5}	0.0 T
Dodecapole	*3.7×10^{6} m^{-6}*	15,460 m^{-6}	0.908 mT
20-pole (k9)	*1.4×10^{15} m^{-10}*	1.7×10^{13} m^{-10}	0.174 mT
28-pole (k13)	*3.7×10^{24} m^{-14}*	5.1×10^{22} m^{-14}	0.039 mT

N.B. all values given are positive, no distinction is given to ±k.
Main k in red bold, allowed harmonics in red italics.

Extraction Octupole

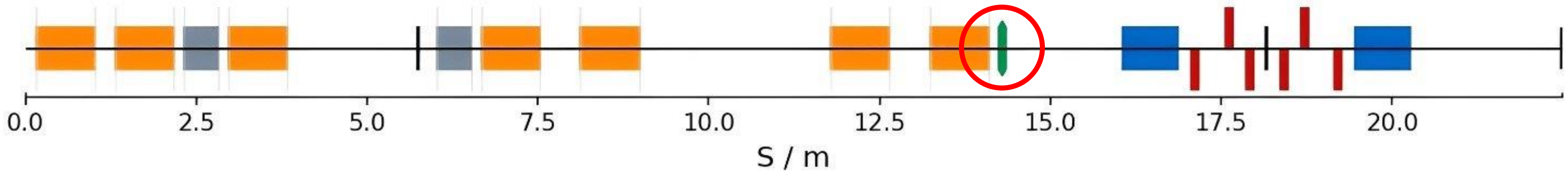

Initial requirements:

- $K_3 \geq 60{,}000\ m^{-4}$
- $B_{max} \leq 2.0$ T
- GFR field purity ≥ 99.9%

Coil Parameters	
Coil Area	3431 mm^2
Current Density	2.48 Amm^{-2}
Turns	10
Cooling Method	Water cooled

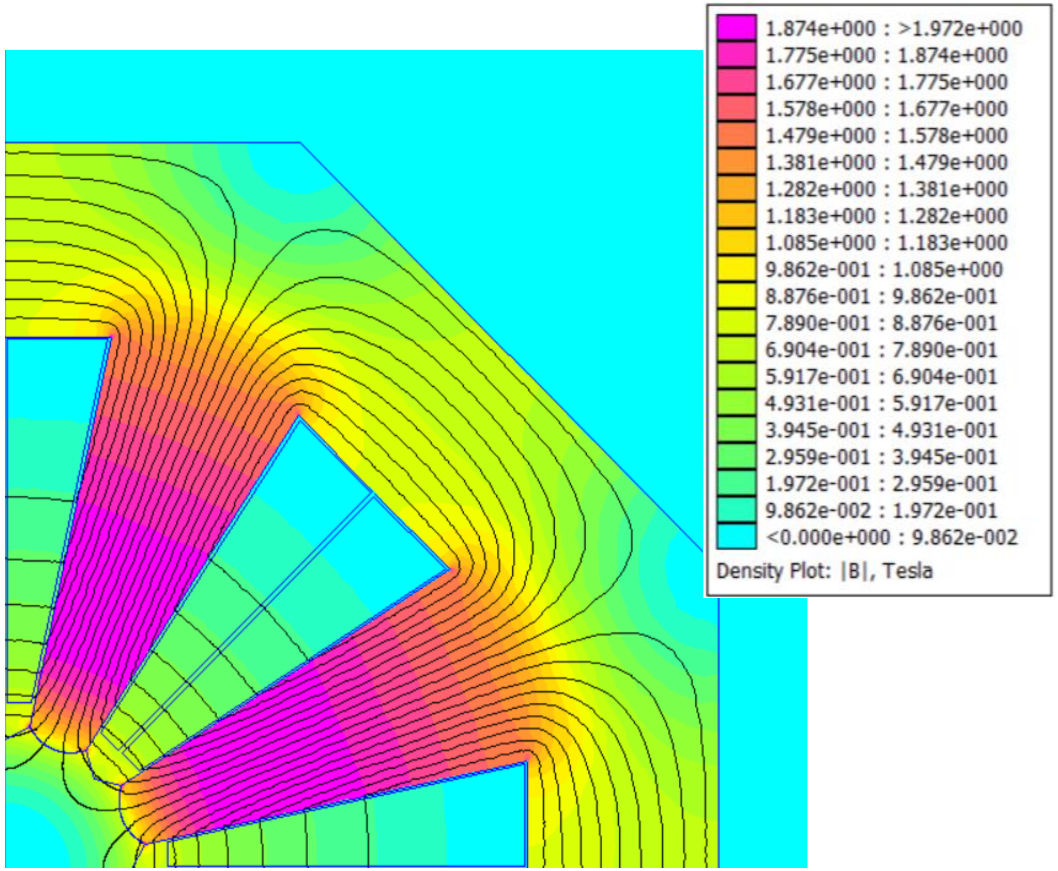

FEMM 4.2 output of ¼-octupole magnet B-field, mesh size 0.03mm

Magnet Design

Octupole GFR Field

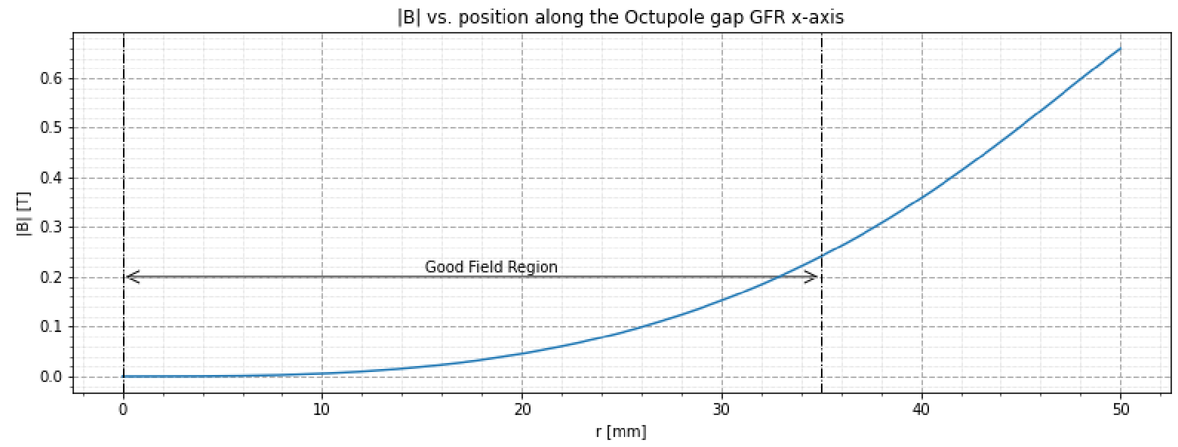

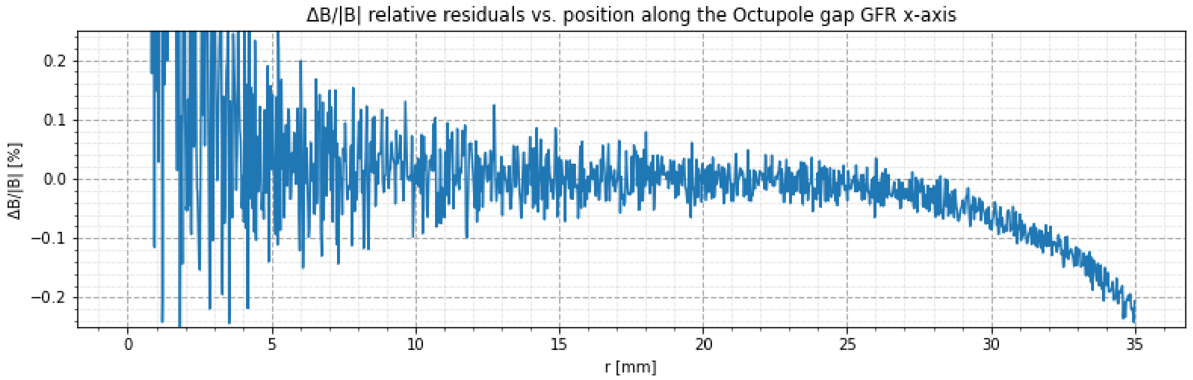

Octupole fitted with calculated $\mathbf{k_3 = 60273m^{-4}}$

Relative **residuals <0.1%** up until edge of GFR (maximum 0.2%)

Octupole Field Analysis

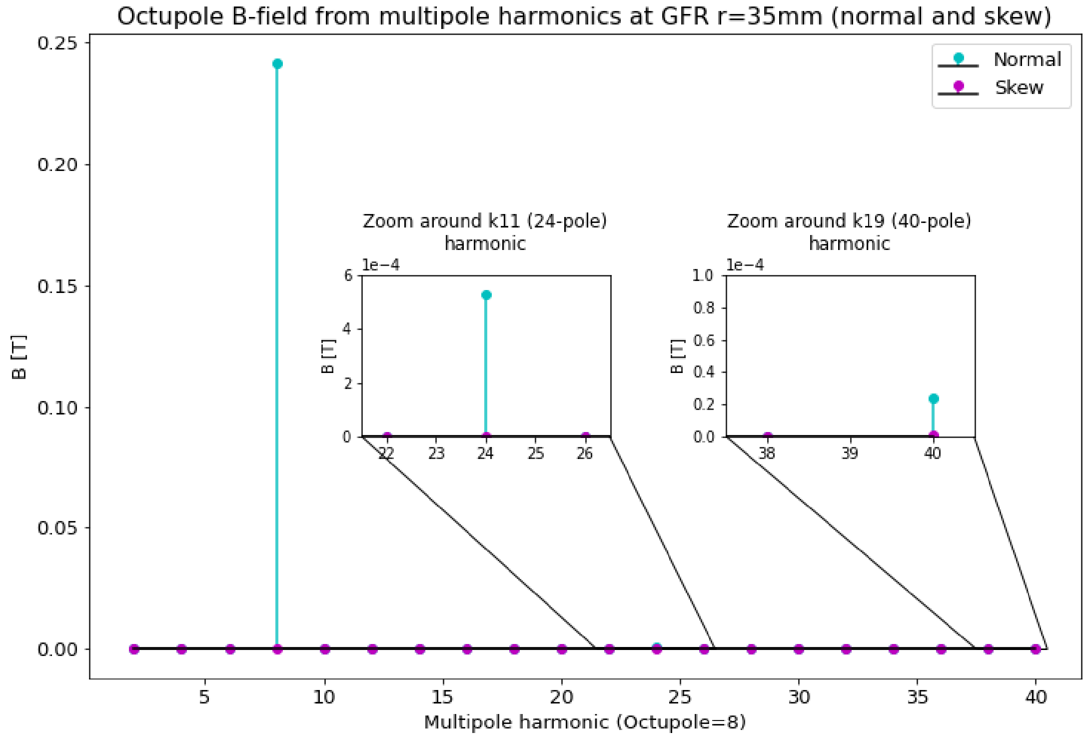

Harmonic	K-value (normal)	K-value (skew)	$B@R=R_{GFR}$
Dipole	0.0 m^{-1}	0.0 m^{-1}	0.0 T
Quadrupole	0.0 m^{-2}	0.0 m^{-2}	0.0 T
Sextupole	0.0 m^{-3}	0.0 m^{-3}	0.0 T
Octupole	**60,273 m^{-4}**	**0.1667 m^{-4}**	**0.242 T**
Decapole	0.0 m^{-5}	0.0 m^{-5}	0.0 T
Dodecapole	0.0 m^{-6}	0.0 m^{-6}	0.0 T
24-pole (k11)	*3.9×10^{20} m^{-12}*	2.4×10^{17} m^{-12}	0.527 mT
40-pole (k19)	*2.4×10^{40} m^{-20}*	7.9×10^{38} m^{-20}	0.024 mT

N.B. all values given are positive, no distinction is given to ±k
Main k in red bold, allowed harmonics in red italics.

Magnet Design

Permanent Magnet Quadrupole Design

- Immediately after the laser ion/proton source the beam is extremely small leading to significant space charge effects.
- A focusing element at very near to the source could allow for more beam to be captured.
- The element must be small, high gradient and radiation hard....

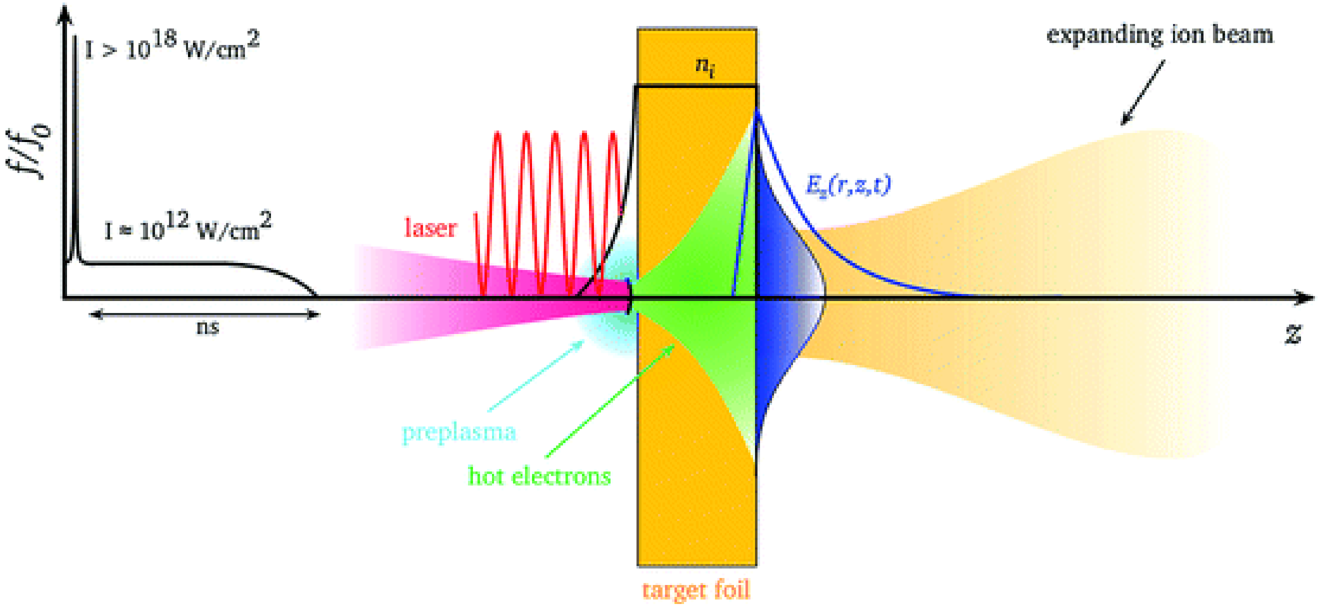

Permanent Magnet Quadrupole Design

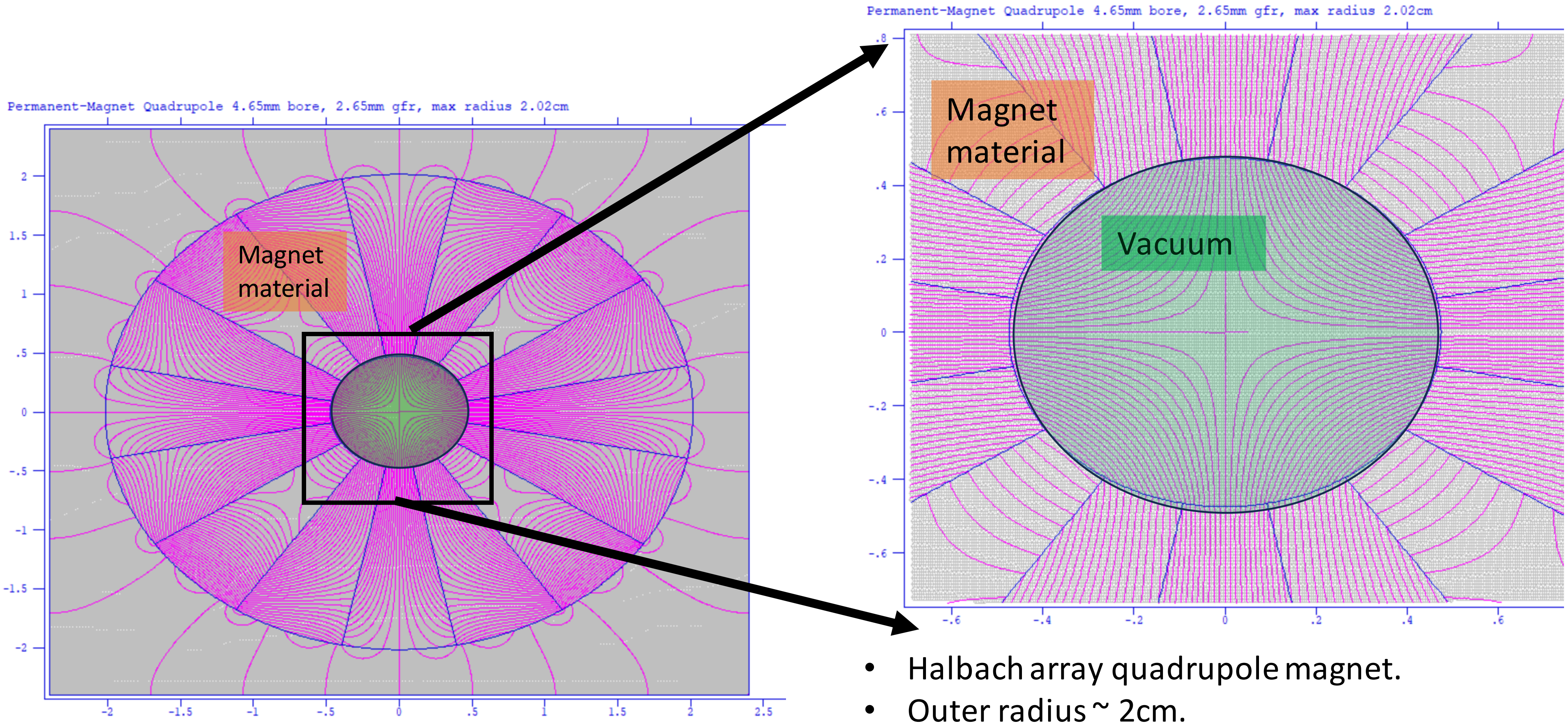

- Halbach array quadrupole magnet.
- Outer radius ~ 2cm.
- Samarium–cobalt magnet material.

Magnet Design

Permanent Magnet Quadrupole Design

Aperture

Field gradient

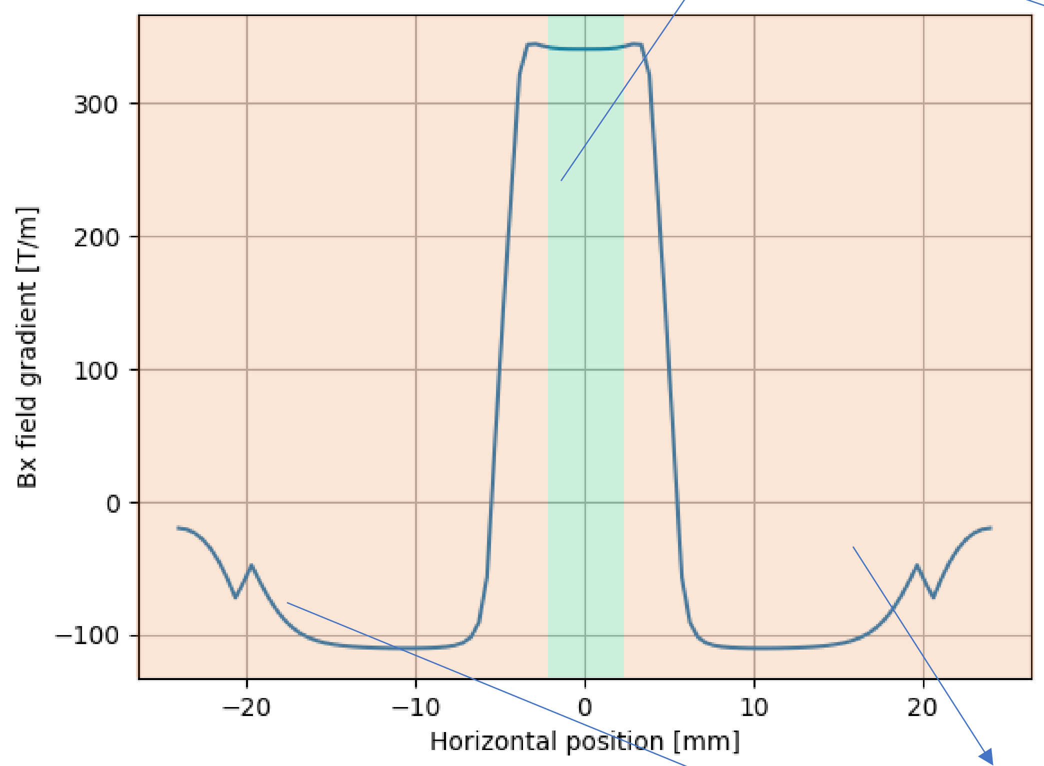

Relative to 340 T/m

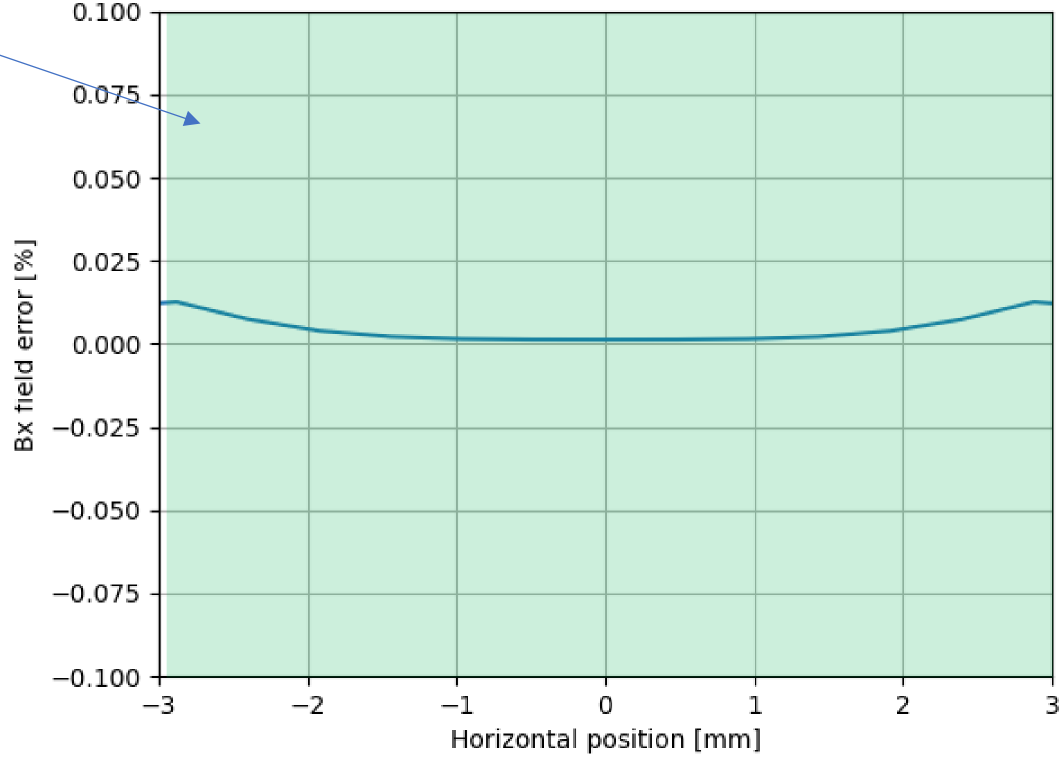

Magnet material

John Adams Institute for Accelerator Science

Summary

Lattice Design:

- Optimised configurations for spot sizes 3.0-1.0 cm
- Performance comparison between Gabor lenses and solenoids
- Quantified beam losses and end station dose rate
- Demonstrated the effect of the octupole on beam uniformity

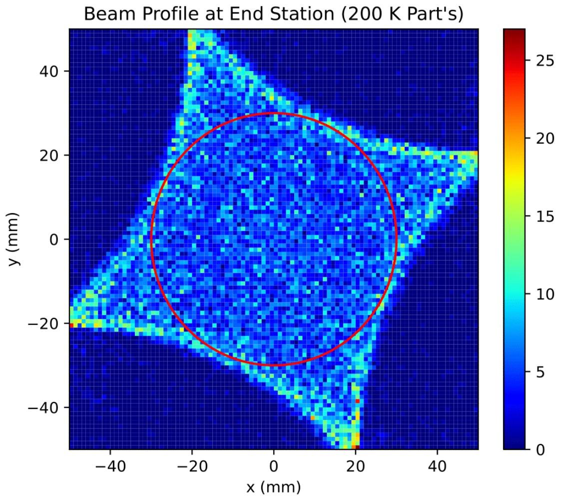

Cavity Design:

- 2D cavity geometry optimisation
- Particle tracking for bunching measurements
- 3D modelling using CST
- Phase-space comparison to BDSim

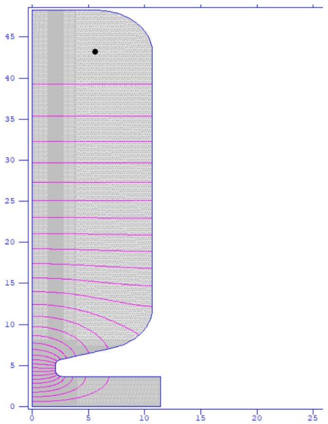

Magnet Design:

- 2D magnet design for dipoles, quadrupoles, octupole and PMQ
- Fourier harmonic analysis

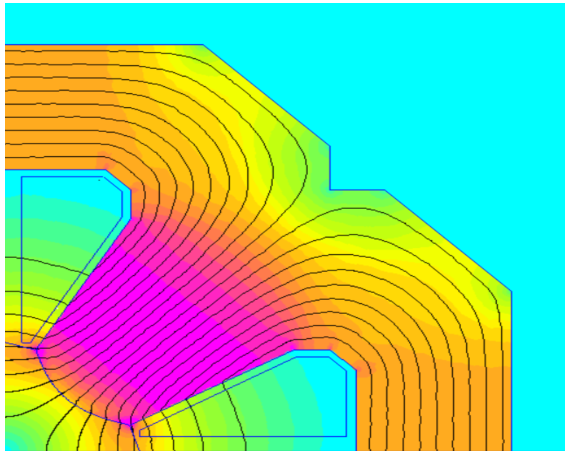

Report:

- Further details are contained in our report.
- Not currently publicly available. Released soon?

Acknowledgements

We would like to extend our deepest gratitude to the many people who gave up their time to assist us in this project, including:

- Emmanuel Tsesmelis
  University of Oxford, John Adams Institute for Accelerator Science|

- William Shields
  Royal Holloway University of London, John Adams Institute for Accelerator Science

- Kenneth Long
  Imperial College London

- Ciprian Plostinar
  European Spallation Source, John Adams Institute for Accelerator Science

- Hossein Ghasem
  Diamond Light Source

We are especially grateful for the many other lecturers of the John Adams Institute Accelerator Physics course, as well as to our PhD supervisors for their generous support.

Bibliography

1. "Figure 1. Comparison of the Radiation Dose as Function of the Depth In..." ResearchGate, ResearchGate, 2020, www.researchgate.net/figure/Comparison-of-the-radiation-dose-as-function-of-the-depth-in-tissue-for-X-rays_fig5_230912423. Accessed 8 Mar. 2024.

2. Hageman, Eline, et al. "Radiobiological Aspects of FLASH Radiotherapy." *Biomolecules*, vol. 12, no. 10, 26 Sept. 2022, pp. 1376–1376, www.mdpi.com/2218-273X/12/10/1376, https://doi.org/10.3390/biom12101376. Accessed 14 Mar. 2024.

3. Aymar, Galen, et al. "LhARA: The Laser-Hybrid Accelerator for Radiobiological Applications." Frontiers in Physics, vol. 8, 29 Sept. 2020, www.frontiersin.org/articles/10.3389/fphy.2020.567738/full, https://doi.org/10.3389/fphy.2020.567738. Accessed 8 Mar. 2024.

4. "Figure 2.4: Target Normal Sheath Acceleration-TNSA. A Thin Target Foil..." ResearchGate, ResearchGate, 2016, www.researchgate.net/figure/Target-Normal-Sheath-Acceleration-TNSA-A-thin-target-foil-with-thickness-d-5-50_fig8_308718768. Accessed 8 Mar. 2024.

5. Gizzi, Leonida A, et al. "Enhanced Laser-Driven Proton Acceleration via Improved Fast Electron Heating in a Controlled Pre-Plasma." *Scientific Reports*, vol. 11, no. 1, 2 July 2021, www.nature.com/articles/s41598-021-93011-3, https://doi.org/10.1038/s41598-021-93011-3. Accessed 14 Mar. 2024.

6. Palkovic, J.A., Mills, F.E., Schmidt, C., & Young, D.E. (1989). Gabor lens focusing of a negative ion beam (FNAL/C--89/115). United States

7. Kurup, A. & Long, K (2020) "LhARA: world-leading radiobiology and novel technology development" https://www.imperial.ac.uk/news/198093/lhara-world-leading-radiobiology-novel-technology-development/ Accessed 13 Mar. 2024.

8. L.J. Nevay et al., BDSIM: An Accelerator Tracking Code with Particle-Matter Interactions, Computer Physics Communications **252** 107200 (2020).

9. Powell, M.J.D. (1994). A Direct Search Optimization Method That Models the Objective and Constraint Functions by Linear Interpolation. In: Gomez, S., Hennart, JP. (eds) Advances in Optimization and Numerical Analysis. Mathematics and Its Applications, vol 275. Springer, Dordrecht. https://doi.org/10.1007/978-94-015-8330-5_4

10. D. C. Meeker, Finite Element Method Magnetics, Version 4.2 (28Feb2018 Build), https://ww.femm.info

MADX Matching and Optimisation

Varying Gabor Lens and Quadrupole strength to achieve smallest possible beam size

```
MATCH, SEQUENCE=lhara, betx=init_betx, bety=init_bety, alfx=init_alfx, alfy=init_alfy;
vary, name = LHA_LEL_MAG_QUAD_01->k1, step=1, lower=-33, upper=-15; // Vary k in gabor lens 4
vary, name = LHA_LEL_MAG_QUAD_02->k1, step=1, lower=10, upper=30; // Vary k in gabor lens 5
vary, name = LHA_LEL_MAG_QUAD_03->k1, step=1, lower=-33, upper=-15; // Vary k in gabor lens 6
vary, name = LHA_LEL_MAG_QUAD_04->k1, step=1, lower=-33, upper=-10; // Vary k in gabor lens 7
vary, name = LHA_LEL_MAG_QUAD_05->k1, step=1, lower=10, upper=33; // Vary k in gabor lens 7
vary, name = LHA_LEL_MAG_QUAD_06->k1, step=1, lower=-33, upper=-15; // Vary k in gabor lens 7
constraint, sequence=lhara, range = LHA_LEL_DIA_COL_04, dy>3.3; // Dispersion high in collimator
constraint, sequence=lhara, range = LHA_LEL_DIA_COL_04, bety<60; // Dispersion = 0 before arc
//constraint, sequence=lhara, range = LHA_LEL_DIA_COL_04, bety<60; // Dispersion = 0 before arc
constraint, sequence=lhara, range = LHA_LEL_VAC_DRI_30, bety<betaY; // Reduce Size at end station
constraint, sequence=lhara, range = LHA_LEL_VAC_DRI_30, betx<betaX; //^^^^^^^^^^
constraint, sequence=lhara, range = LHA_LEL_VAC_DRI_30, alfy=0; //Alfa 0 at end station
constraint, sequence=lhara, range = LHA_LEL_VAC_DRI_30, alfx=0;//^^^^^^^^^^
constraint, sequence=lhara, range = LHA_LEL_VAC_DRI_30, dy=0;// Dispersion = 0 at end station
constraint, sequence=lhara, range = LHA_LEL_VAC_DRI_30, dx=0;//^^^^^^^^^^
```

DOF

Constraints

Uses sum of squares of constraint functions